bioRxiv preprint doi: https://doi.org/10.1101/2020.09.05.284422; this version posted January 11, 2021. The copyright holder for this preprint (which was not certified by peer review) is the author/funder, who has granted bioRxiv a license to display the preprint in perpetuity. It is made available under aCC-BY-NC-ND 4.0 International license.

High-content analysis and Kinetic Image Cytometry identify toxic and epigenotoxic effects of HIV antiretrovirals on human iPSC-neurons and primary neural precursor cells

Alyson S. Smith[1], Soneela Ankam[1], Chen Farhy[2], Lorenzo Fiengo[2], Ranor C.B. Basa[1], Kara L. Gordon[1], Charles T. Martin[1], Alexey V. Terskikh[2], Kelly L. Jordan-Sciutto[3,4], Jeffrey H. Price[1,5], Patrick M. McDonough[1]

[1]Vala Sciences, Inc., San Diego, CA; [2]Sanford Burnham Prebys Medical Discovery Institute, La Jolla, CA; [3]Department of Pathology, Perelman School of Medicine, University of Pennsylvania, Philadelphia, PA; [4]Department of Basic and Translational Sciences, School of Dental Medicine, University of Pennsylvania, Philadelphia, PA; [5]Scintillon Institute, San Diego, CA

To whom correspondence should be addressed: asmith@valasciences.com

bioRxiv preprint doi: https://doi.org/10.1101/2020.09.05.284422; this version posted January 11, 2021. The copyright holder for this preprint (which was not certified by peer review) is the author/funder, who has granted bioRxiv a license to display the preprint in perpetuity. It is made available under aCC-BY-NC-ND 4.0 International license.

Abstract

Despite viral suppression due to combination antiretroviral therapy (cART), HIV-associated neurocognitive disorders (HAND) continue to affect half of people with HIV, suggesting that certain antiretrovirals (ARVs) may contribute to HAND. We examined the effects of nucleoside/nucleotide reverse transcriptase inhibitors tenofovir disproxil fumarate (TDF) and emtricitabine (FTC) and the integrase inhibitors dolutegravir (DTG) and elvitegravir (EVG) on viability, structure, and function of glutamatergic neurons (a subtype of CNS neuron involved in cognition) derived from human induced pluripotent stem cells (hiPSC-neurons), and primary human neural precursor cells (hNPCs), which are responsible for neurogenesis. Using automated digital microscopy and image analysis (high content analysis, HCA), we found that DTG, EVG, and TDF decreased hiPSC-neuron viability, neurites, and synapses after seven days of treatment. Analysis of hiPSC-neuron calcium activity using Kinetic Image Cytometry (KIC) demonstrated that DTG and EVG also decreased the frequency and magnitude of intracellular calcium transients. Longer ARV exposures and simultaneous exposure to multiple ARVs increased the magnitude of these neurotoxic effects. Using the Microscopic Imaging of Epigenetic Landscapes (MIEL) assay, we found that TDF decreased hNPC viability and changed the distribution of histone modifications that regulate chromatin packing, suggesting that TDF may reduce neuroprogenitor pools important for CNS development and maintenance of cognition in adults. This study establishes human preclinical assays that can screen potential ARVs for CNS toxicity to develop safer cART regimens and HAND therapeutics.

Keywords: Human induced pluripotent stem cell-derived glutamatergic neurons; human neural precursor cells; HIV antiretrovirals; HIV-associated neurocognitive disorder; high content analysis; kinetic image cytometry; calcium transients; neurites; synapses; epigenetic regulation

bioRxiv preprint doi: https://doi.org/10.1101/2020.09.05.284422; this version posted January 11, 2021. The copyright holder for this preprint (which was not certified by peer review) is the author/funder, who has granted bioRxiv a license to display the preprint in perpetuity. It is made available under aCC-BY-NC-ND 4.0 International license.

Introduction

About 40 million people live with human immunodeficiency virus (HIV) infection globally, and there are ~1.7 million new infections per year[1]. Combination antiretroviral therapy (cART), which involves simultaneous treatment with 2-4 antiretrovirals (ARVs), suppresses HIV replication, prevents progression to acquired immunodeficiency syndrome (AIDS), and extends life expectancy in adults with HIV to near normal[2,3]. Preexposure prophylaxis with cART can also prevent transmission of HIV to HIV-negative adolescents and adults at risk for behaviorally acquiring HIV[4-8], as well as mother-to-child transmission[9,10]. cART has greatly reduced the incidence of AIDS-defining illnesses that affect the central nervous system (CNS), including opportunistic infections, primary CNS lymphoma, and HIV-associated dementia (HAD)[11-14]. However, the post-cART era has seen increased incidence of milder forms of HIV-associated neurocognitive disorder (HAND), including mild cognitive disorder (MND) and asymptomatic neurocognitive impairment (ANI)[15,16]. HAND affects approximately 50% of people living with HIV, including patients with undetectable viral loads[17,18] and can impact quality of life, employment, treatment adherence, and survival[19-21]. HAND can also increase the risk for progression to more severe cognitive impairment[22,23].

While many factors likely contribute to cognitive impairment in people with HIV on cART, there is growing concern that ARV neurotoxicity contributes[24]. In pigtail macaques, rodents, and cultured rodent neurons, ARV exposure can cause oxidative stress, endoplasmic reticulum stress, mitochondrial dysfunction, loss of neurites and synapses, and/or neuronal cell death[25-28]. In people with HIV, cART can reduce neuronal metabolite levels[29], the volume and structural integrity of cortical white matter[30,31], and cognitive reserve as measured by functional MRI[32]. While some studies link cART regimens with high CNS penetration effectiveness (CPE) with improved cognition[33] or no effect on cognition[34], others link high CPE with worse cognitive outcomes[35,36], including a study with 61,938 people with HIV[37]. Treatment interruption in HIV+ individuals with

bioRxiv preprint doi: https://doi.org/10.1101/2020.09.05.284422; this version posted January 11, 2021. The copyright holder for this preprint (which was not certified by peer review) is the author/funder, who has granted bioRxiv a license to display the preprint in perpetuity. It is made available under aCC-BY-NC-ND 4.0 International license.

stable immune function can also improve neurocognitive performance for extended time periods[38]. People with HIV must remain on cART for their lifetime to maintain viral suppression[39,40], leaving them vulnerable to increased neurotoxicity during neurodevelopment and aging. Indeed, children with HIV receiving cART have reduced cognition[41-43], and HIV-children who received perinatal cART experience developmental delays[44]. cART also increases production and reduces clearance of Alzheimer's disease-associated beta amyloid peptides in vitro[45-47] and in patients[48,49], which may accelerate CNS aging and cognitive decline.

In previous research using HCA and KIC, we found that tamoxifen, an anti-cancer agent linked to post-chemotherapy cognitive impairment, reduces synapses and calcium transient activity of primary rat hippocampal neurons, establishing that these in vitro techniques can test agents for potential negative impacts on cognition[50]. In this study, we aimed to develop human preclinical neurosafety testing platforms to screen ARVs for a broad range of potential neurotoxic and neurodevelopmental effects. We first developed HCA and KIC assays using glutamatergic neurons differentiated from human induced pluripotent stem cells (hiPSC-neurons), which provide an in vitro model system with similar gene expression, cell biology, and electrophysiology to neurons in the human brain in which to test directly for compound toxicity[51-53]. We also developed an assay to test ARVs for potential effects on neurogenesis, a process by which human neural precursor cells (hNPCs) differentiate to neurons to support central nervous system development and cognitive function in adults[54,55]. For this, we used the MIEL assay, a multiparametric approach to identify changes in histone acetylation and methylation patterns using HCA of immunofluorescence images[56].

Using HCA and KIC methods on hiPSC-neurons, we found that the nucleoside/nucleotide reverse transcriptase inhibitors tenofovir disproxil fumarate (TDF) and emtricitabine (FTC) and the integrase inhibitors dolutegravir (DTG) and elvitegravir (EVG) altered key neuronal structures and functions to varying extents, and that combinations of these ARVs had additive effects.

bioRxiv preprint doi: https://doi.org/10.1101/2020.09.05.284422; this version posted January 11, 2021. The copyright holder for this preprint (which was not certified by peer review) is the author/funder, who has granted bioRxiv a license to display the preprint in perpetuity. It is made available under aCC-BY-NC-ND 4.0 International license.

Additionally, the MIEL assay showed that TDF reduced viability and altered histone acetylation and methylation in hNPCs, indicating an epigenotoxic effect. Our findings suggest novel preclinical research strategies to test candidate ARVs in vitro and to aid in identifying ARVs with reduced neurocognitive effects.

bioRxiv preprint doi: https://doi.org/10.1101/2020.09.05.284422; this version posted January 11, 2021. The copyright holder for this preprint (which was not certified by peer review) is the author/funder, who has granted bioRxiv a license to display the preprint in perpetuity. It is made available under aCC-BY-NC-ND 4.0 International license.

Materials and Methods

Cell Culture. For hiPSC-neuron experiments, imaging-quality polystyrene 384-well plates (Greiner Bio-One #781090; Frickenhausen, Germany) were coated with 0.1% polyethyleneimine and 0.028 mg/mL growth factor-reduced Matrigel (Corning Life Sciences #354230, Tewksbury, MA, USA). hiPSC-derived glutamatergic neurons (iCell GlutaNeurons; Fujifilm CDI #C1060, Madison, WI, USA) were seeded at a density of 60,000 live cells/cm^2 and were maintained per the manufacturer's instructions for a total of 14 days before assay.

For hNPC experiments, imaging-quality polystyrene 384-well plates (Greiner Bio-One #781090; Frickenhausen, Germany) were coated with 0.028 mg/mL growth factor-reduced Matrigel (Corning Life Sciences #354230, Tewksbury, MA, USA). Fetal hNPCs (Thermo Fisher Scientific # A15654; Waltham, MA, USA) were seeded at a density of 18,200 live cells/cm^2 and were maintained in differentiation medium per the manufacturer's instructions for a total of 7 days before assay.

Test Compounds. hiPSC-neuron cultures were treated with ARVs or ARV combinations for 1 or 7 days prior to assays. The following ARVs were used alone or in combination in this study: dolutegravir (DTG; Toronto Research Chemicals #D528800; Toronto, ON, Canada), elvitegravir (EVG; Toronto Research Chemicals #E509000), tenofovir disproxil fumarate (TDF; Toronto Research Chemicals #T018505), emtricitabine (FTC; Toronto Research Chemicals #E525000), DTG+TDF+FTC, EVG+TDF+FTC, and TDF+FTC. Vehicle (0.2% DMSO) and antagonist control treatments (25 µM *para*-nitroblebbistatin; Optopharma Ltd. #DR-N-111; Budapest, Hungary) were also applied to the cells. hNPCs were treated with 0.2% DMSO, ARVs, SAHA (Cayman Chemical #10009929; Ann Arbor, MI, USA), GSK343 (Cayman Chemical #14094), tofacitinib (TOF, Cayman Chemical #11598), or (+)-JQ1 (Cayman Chemical #11187).

bioRxiv preprint doi: https://doi.org/10.1101/2020.09.05.284422; this version posted January 11, 2021. The copyright holder for this preprint (which was not certified by peer review) is the author/funder, who has granted bioRxiv a license to display the preprint in perpetuity. It is made available under aCC-BY-NC-ND 4.0 International license.

Automated Microscopy. The fixed-endpoint synapse and neurite length assay and microscopic imaging of the epigenetic landscape (MIEL) assay, as well as the live-cell calcium KIC assay were imaged using the IC200-KIC automated microscope (Vala Sciences Inc.; San Diego, CA, USA; Kinetic Image Cytometry® and KIC® are registered trademarks of Vala Sciences Inc.) outfitted with a Plan Apo 20X/0.75 NA objective lens (Nikon Instruments Inc.; Melville, NY, USA). For live-cell assays, the environmental chamber of the IC200-KIC was set to 37°C/5% CO_2.

Synapse Density and Neurite Length Assay. After treatment, cells were fixed in 2% paraformaldehyde/1.67% sucrose in HBSS without Ca^{++}/Mg^{++}, permeabilized in 0.3% Triton X-100 in PBS with Ca^{++}/Mg^{++}, and blocked in 5% normal goat serum/1% BSA/0.1% Triton X-100. The following primary antibodies were diluted in blocking buffer and applied to cells overnight at 4°C: chicken anti-βIII tubulin (Tuj-1, 1:200; Abcam #ab41489; Boston, MA, USA), rabbit anti-PSD95 (1:200; Thermo Fisher Scientific #51-6900; Waltham, MA, USA), and mouse anti-SV2 (1:150; Developmental Studies Hybridoma Bank; Iowa City, IA, USA). The next day, the following secondary antibody cocktail with Hoechst nuclear stain was made in 2% BSA and applied to the cells for 1 hour at room temperature in the dark: goat anti-chicken IgY Alexa Fluor 555 (1:500; Thermo Fisher Scientific #A21437), goat anti-rabbit IgG Alexa Fluor 647 (1:500; Thermo Fisher Scientific #A21245), goat anti-mouse IgG Alexa Fluor 488 (1:500; Thermo Fisher Scientific #A11029), and 10 µg/mL Hoechst 33342 (Thermo Fisher Scientific #H3570). For each well, a 3-by-3 matrix of images was acquired in each optical channel.

Calcium KIC Assay. Neurons were incubated in a calcium indicator dye solution consisting of 5 µM Rhod-4 AM (AAT Bioquest #21122; Sunnyvale, CA, USA), 1X PowerLoad (Thermo Fisher Scientific #P10020), 1 µg/mL Hoechst 33342, and 2.5 mM probenecid in phenol red-free BrainPhys (Stemcell Technologies #05791; Vancouver, BC, Canada) for 40 min at 37°C. The neurons were then rinsed with and imaged under phenol red-free BrainPhys. The calcium indicator dye solution and the imaging media did not contain DMSO or ARVs. One field of view

bioRxiv preprint doi: https://doi.org/10.1101/2020.09.05.284422; this version posted January 11, 2021. The copyright holder for this preprint (which was not certified by peer review) is the author/funder, who has granted bioRxiv a license to display the preprint in perpetuity. It is made available under aCC-BY-NC-ND 4.0 International license.

was imaged per well, including a single image in the nuclear channel followed by a calcium movie acquired at 4 frames per second for 2 minutes.

hNPC Microscopic Imaging of Epigenetic Landscape (MIEL) Assay. After treatment, cells were fixed in 2% paraformaldehyde/1.67% sucrose in HBSS without Ca^{++}/Mg^{++} and blocked/permeabilized in PBS with Ca^{++}/Mg^{++} and 2% BSA/0.5% Triton X-100. The following primary antibodies were diluted in blocking buffer and applied to cells overnight at 4°C to label key histone modifications associated with epigenetic regulation: rabbit H3K9me3 (1:500; Active Motif, 39765; Carlsbad, CA, USA); mouse H3K4me1 (1:100; Active Motif, 39635; Carlsbad, CA, USA); mouse H3K27me3 (1:250; Active Motif, 61017; Carlsbad, CA, USA); and rabbit H3K27ac (1:500; Active Motif, 39133; Carlsbad, CA, USA). Two sets of cells were immunolabeled for the biomarkers: one set with H3K27me3 and H3K27ac and a second set with H3K9me3 and H3K4me1. The next day, the following secondary antibody cocktail with Hoechst nuclear stain was made in 2% BSA and applied to the cells for 1 hour at room temperature in the dark: goat anti-rabbit IgG Alexa Fluor 647 (1:500; Thermo Fisher Scientific #A21245), goat anti-mouse IgG Alexa Fluor 488 (1:500; Thermo Fisher Scientific #A11029), and 10 µg/mL Hoechst 33342 (Thermo Fisher Scientific #H3570).

Automated Image Analysis. For hiPSC-neuron synapse density, neurite length, and calcium KIC assays, images were analyzed using custom algorithms in CyteSeer software (Vala Sciences Inc.; CyteSeer® is a registered trademark of Vala Sciences Inc.). The NO2 v7.2.4 Neurite Morphology and Synapse Density with Somas algorithm was used to analyze the synapse density and neurite length images. This algorithm identified live neuronal nuclei as relatively large nuclei with diffuse Hoechst staining (as opposed to small, bright, dead nuclei) that colocalize with neuron-specific βIII-tubulin (Tuj-1) staining. The algorithm then identified Tuj-1+ neurites, which includes axons and dendrites. Small neurite fragments and Tuj-1+ cellular debris were excluded, as well as the Tuj-1 positive neuronal cell bodies (somas). To identify synapses, the algorithm

bioRxiv preprint doi: https://doi.org/10.1101/2020.09.05.284422; this version posted January 11, 2021. The copyright holder for this preprint (which was not certified by peer review) is the author/funder, who has granted bioRxiv a license to display the preprint in perpetuity. It is made available under aCC-BY-NC-ND 4.0 International license.

first identified SV2+ (presynaptic) and PSD95+ (postsynaptic) puncta with areas between 0.32 and 1.27 μm^2 (between 3 and 15 $pixels^2$ with a pixel size of 0.325 µm). To be considered synapses, the SV2+ puncta centroids were required to be within 1.95 µm (6 pixels) of the nearest neurite and within 0.975 µm (3 pixels) of the nearest PSD95+ puncta centroid. Neuronal viability, neurite, and synapse data are presented as one data point per well, with each data point representing the average value across each of the 9 fields of view acquired per well. Each field of view contained about 200 live neurons in DMSO-treated control wells.

The calcium KIC assays were analyzed with the Neuron Calcium KIC v10.5 algorithm. Neuronal cell bodies were identified as Rhod-4 AM-positive areas associated with live neuron nuclei. The average pixel intensity of Rhod-4 AM signal in each cell body was measured for each of the 480 frames (4 frames per second for two minutes). The resulting functions of Rhod-4 AM average pixel intensity over time were baseline subtracted to determine if each neuron displayed calcium transients during the recording period and to calculate the event frequencies and mean peak amplitudes for each active cell. Event frequency and mean peak amplitude data are presented as one data point per well, with each data point representing the average value of all active neurons in each field of view. Each field of view contained about 200 live neurons in DMSO-treated control wells.

For the MIEL assay, images were analyzed using Acapella 2.6 (PerkinElmer), and image texture features were analyzed as described in Farhy, et al., eLife, 2019[56]. Quadratic discriminant analysis was performed on histone modification texture features using the Excel add-on program Xlstat (Base, v19.06).

Statistical Analysis. The data were analyzed with Prism (GraphPad Software; San Diego, CA, USA) using ANOVA, followed by either Dunnett's or Tukey's post-hoc multiple comparisons test for statistical significance (*p<0.05, **p<0.01, ***p<0.001).

bioRxiv preprint doi: https://doi.org/10.1101/2020.09.05.284422; this version posted January 11, 2021. The copyright holder for this preprint (which was not certified by peer review) is the author/funder, who has granted bioRxiv a license to display the preprint in perpetuity. It is made available under aCC-BY-NC-ND 4.0 International license.

Results

HCA to characterize HIV ARV effects on neuronal viability and neurites in hiPSC-neurons. To test for ARV neurotoxicity, we exposed hiPSC-neurons to 0.1, 1, or 10 µM of DTG, EVG, TDF, or FTC for seven days. We chose these concentrations to test for neurotoxic effects at levels below, near, and above the plasma Cmax of each ARV (Table 1). We used 25 µM blebbistatin, a nonmuscle myosin II inhibitor[57,58], as a control compound. We then fixed the hiPSC-neurons and immunolabeled for Tuj-1 (neuron-specific βIII-tubulin), SV2 (presynaptic protein), PSD95 (postsynaptic protein), stained with Hoechst (nuclei), and imaged the cells with the IC200 Image Cytometer to assess neuronal viability and morphology. Images of Tuj-1 and nuclei show significant loss of neurites in hiPSC-neurons treated with 10 µM EVG, indicating a neurotoxic effect, with smaller effects for the other ARVs (Fig. 1A). Image analysis with a CyteSeer algorithm that identifies the nuclei corresponding to live neurons (see Methods) determined that Neuronal Viability (the percentage of live neuronal nuclei) was significantly reduced by 30% at 10 µM DTG, 65% at 10 µM EVG, and 35% at 10 µM TDF (Fig. 1B). We did not observe changes in Neuronal Viability at lower concentrations of TDG, EVG, or TDF, or at any tested concentration of FTC.

To further quantify effects of the ARVs, we used a CyteSeer image analysis algorithm that traces Tuj-1-positive neurites and calculates their length. The total neurite length per cm^2 image area (Total Neurite Length) was significantly reduced by 20% at 10 µM DTG, 80% at 10µM EVG, and 20% at 10µM TDF (Fig. 1C). The Neurite Length per Neuron (Total Neurite Length divided by the number of live neuronal nuclei) was slightly but significantly increased by 20% ($p < 0.05$) after treatment with 10 µM DTG but was 50% lower after treatment with 10 µM EVG (Fig. 1D). The Total Neurite Length and Neurite Length per Neuron remained similar to DMSO alone at lower concentrations of DTG, EVG, and TDF, and at all tested concentrations of FTC.

bioRxiv preprint doi: https://doi.org/10.1101/2020.09.05.284422; this version posted January 11, 2021. The copyright holder for this preprint (which was not certified by peer review) is the author/funder, who has granted bioRxiv a license to display the preprint in perpetuity. It is made available under aCC-BY-NC-ND 4.0 International license.

Most HIV infections are treated with combination antiretroviral therapy (cART) consisting of two, three, or four ARVs from two or more different classes[2-4]. To test whether cART causes increased neurotoxicity and neurite loss compared to single ARVs, we compared Neuronal Viability and neurite length measurements in hiPSC-neurons treated with 10 µM DTG, EVG, TDF, FTC, or three combinations (DTG/TDF/FTC, EVG/TDF/FTC, or TDF/FTC; all ARVs at 10 µM). DTG/TDF/FTC has been the primary cART regimen in use in Botswana since 2016 for all people with HIV, including pregnant women[59]. TDF/FTC and EVG/TDF/FTC are components of Truvada and Stribild, respectively (made by Gilead Sciences, Stribild also features cobicistat).

Treatment with single or combination ARVs for one day did not affect Neuronal Viability, Total Neurite Length, or Neurite Length per Neuron (Fig. 2A-C), although blebbistatin increased Total Neurite Length by 15% (Fig. 2B). By contrast, seven-day ARV and cART exposure caused significant neurotoxicity. Neuronal Viability was significantly reduced by 20% by 10 µM DTG, 80% by 10 µM EVG, 30% by 10µM TDF, 70% by DTG/TDF/FTC, 85% by EVG/TDF/FTC, and 30% by TDF/FTC (Fig. 2D). We used the Tukey's multiple comparisons test to test for significant differences between data from all test conditions and the DMSO control and between single ARVs to the ARV combinations (see Supplemental Data for full results). Comparing ARV combinations to their components, TDF/FTC treatment led to similar Neuronal Viability to that of TDF alone, suggesting FTC does not affect TDF toxicity (Table S1). EVG/TDF/FTC treatment also led to similar Neuronal Viability to that of EVG alone, suggesting that TDF and FTC do not affect EVG toxicity. By contrast, DTG/TDF/FTC treatment significantly reduced Neuronal Viability compared to either DTG alone or TDF/FTC ($p<0.001$ for both comparisons), suggesting additive toxicity by these ARVs.

Seven-day ARV exposure also significantly reduced Total Neurite Length for hiPSC-neurons treated with 10 µM EVG (85% reduction), DTG/TDF/FTC (55%), and EVG/TDF/FTC (90%) (Fig. 2E). DTG/FTC/TDF treatment led to a 50% lower Total Neurite Length than DTG

bioRxiv preprint doi: https://doi.org/10.1101/2020.09.05.284422; this version posted January 11, 2021. The copyright holder for this preprint (which was not certified by peer review) is the author/funder, who has granted bioRxiv a license to display the preprint in perpetuity. It is made available under aCC-BY-NC-ND 4.0 International license.

alone ($p<0.001$), while EVG/TDF/FTC treatment led to a similar neurite length to that of EVG alone. Neurite lengths were similar to DMSO for hiPSC-neurons treated with TDF, FTC, or TDF/FTC. Neurite Length per Neuron did not change significantly with any ARV treatment, but there was increased variability in wells treated with EVG, DTG/TDF/FTC, and EVG/TDF/FTC (Fig. 2F). See Tables S2 and S3 for the results of comparisons between each condition for Total Neurite Length and Neurite Length per Neuron.

For both Neuronal Viability and Total Neurite Length, EVG displayed dominant neurotoxic effects in combination treatments (EVG alone reduced Neuronal Viability and Total Neurite Length to the same degree as EVG/TDF/FTC), while DTG and TDF had additive effects (DTG/TDF/FTC reduced Neuronal Viability and Total Neurite Length to a greater extent than either DTG or TDF/FTC).

HCA to characterize HIV ARV effects on synapses in hiPSC-neurons. To measure the effects of ARV treatments on hiPSC-neuron synapses, we used a CyteSeer image analysis algorithm that identifies synapses as SV2 (presynaptic) and PSD95 (postsynaptic) puncta near each other and Tuj-1-positive neurites. We defined Synapse Density as the number of synapses per cm^2 of the imaging area and Synapses/Neurite Length as the number of synapses per Total Neurite Length (in microns). Figure 3A shows representative images of SV2 (left) and PSD95 (center) staining of hiPSC-neurons exposed to ARVs for seven days and the live neuronal nuclei (green), neurites (cyan), and synapses (magenta) identified by CyteSeer (right). hiPSC-neurons treated with 10 µM EVG had fewer synapses, with smaller effects for the other ARVs. Effects on hiPSC-neuron synapses appeared at lower doses and for more ARVs than the effects on neuronal viability and neurite length. Synapse Density was significantly reduced by 1 µM DTG (30%), 0.1 µM (20%) and 10 µM (75%) EVG, 1 µM (30%) and 10 µM (40%) TDF, 1 µM (20%) and 10 µM (30%) FTC, and blebbistatin (30%) (Fig. 3B). DTG significantly reduced the Synapses/Neurite Length by 20% at 0.1 µM and 30% at 1 µM but had no effect at 10 µM (Fig. 3C). EVG decreased

bioRxiv preprint doi: https://doi.org/10.1101/2020.09.05.284422; this version posted January 11, 2021. The copyright holder for this preprint (which was not certified by peer review) is the author/funder, who has granted bioRxiv a license to display the preprint in perpetuity. It is made available under aCC-BY-NC-ND 4.0 International license.

the Synapses/Neurite Length by 25% at 0.1 µM, had no effect at 1 µM, and increased the Synapses/Neurite Length by 20% at 10 µM. TDF and FTC reduced the Synapses/Neurite Length at all tested concentrations (20%, 25%, and 20% for 0.1, 1, and 10 µM TDF and 20%, 20%, and 30% for 0.1, 1, and 10 µM FTC). Blebbistatin reduced the Synapses/Neurite Length by 20%.

In experiments comparing 10 µM doses of single ARVs to ARV combinations, one-day treatments did not affect the Synapse Density or Synapses/Neurite Length, although blebbistatin increased the Synapse Density by 20% (Fig 4A, B). By contrast, the Synapse Density was significantly reduced by seven-day treatment with EVG (90%), DTG/TDF/FTC (60%), EVG/TDF/FTC (90%), and TDF/FTC (20%) (Fig. 4C). DTG/FTC/TDF treatment led to a 50% lower Synapse Density than that of DTG alone ($p<0.001$, Tukey's), while EVG/TDF/FTC treatment led to a similar Synapse Density to that of EVG alone. TDF/FTC treatment reduced the Synapses/Neurite Length by 20% (vs. DMSO, $p<0.001$), but this parameter was not affected by other ARV treatments (Fig. 4D). See Tables S4 and S5 for the results of comparisons between each condition for Synapse Density and Synapses/Neurite Length.

KIC to characterize HIV ARV effects on intracellular calcium transients in hiPSC-neurons. Neurons exhibit action potential-dependent and -independent peaks in intracellular calcium concentration that induce molecular and structural changes within neurons through calcium-sensitive effectors[60-62]. Dysregulation of neuronal intracellular calcium concentration and signaling occurs in aging, traumatic brain injury, and neurodegenerative diseases[63]. To test ARVs for effects on neuronal calcium transients, we treated hiPSC-neurons with 10 µM of each ARV alone or in combination for one or seven days. We then loaded the hiPSC-neurons with Hoechst and the calcium indicator Rhod-4 and assayed the cells for calcium activity. For each well, we collected a single image in the nuclear channel and a digital movie in the Rhod-4 channel at four frames per second for two minutes. We then used a CyteSeer KIC analysis algorithm originally developed for quantifying calcium transients in cardiac myocytes[64] and adapted to quantify neuronal calcium

bioRxiv preprint doi: https://doi.org/10.1101/2020.09.05.284422; this version posted January 11, 2021. The copyright holder for this preprint (which was not certified by peer review) is the author/funder, who has granted bioRxiv a license to display the preprint in perpetuity. It is made available under aCC-BY-NC-ND 4.0 International license.

transients[50]. The algorithm measured the Rhod-4 signal in the soma associated with each live neuron nucleus at each frame, enabling detection of each calcium transient that occurred in each neuron during the recording period. The algorithm then calculated parameters including the percent of neurons with calcium transients and frequency and amplitude of the transients.

hiPSC-neurons exposed to DMSO alone for 7 days displayed between 0 and 50 calcium transients that were typically 5 to 30 seconds in duration during the two-minute recording periods (Fig. 5A). hiPSC-neurons exposed to TDF, FTC, and TDF/FTC for 7 days displayed similar calcium transient activity to those treated with DMSO alone (Fig. 5D, E, H), while neurons treated with DTG or DTG/TDF/FTC had less calcium transient activity compared to DMSO (Fig. 5B, F) and neurons treated with EVG or EVG/TDF/FTC were virtually inactive (Fig. 5C, G).

Quantification of the calcium transient activity showed no significant effects after one day of ARV exposure (Fig. 6A-C). After seven days of ARV exposure, the percent active hiPSC-neurons was reduced by 30% by DTG, 90% by EVG, 70% by DTG/TDF/FTC, 95% by EVG/TDF/FTC, and 25% by TDF/FTC (Fig. 6D). DTG/TDF/FTC treatment led to 60% lower percent activity than DTG alone ($p<0.001$), while EVG/TDF/FTC treatment led to a similar effect on percent activity to that of EVG alone. The event frequency (Fig. 6E) was significantly reduced by EVG (40%) and by EVG/TDF/FTC (55%), but not by any of the other treatments (while event frequency for DTG/TDF/FTC was lower than for DMSO, this difference did not achieve statistical significance). The mean peak amplitude was also significantly reduced by 10 µM EVG (55%) and EVG/TDF/FTC (50%), but not by any of the other treatments. See Tables S6-8 for the results of comparisons between each condition for percent activity, event frequency, and mean peak amplitude.

Microscopic imaging of the epigenetic landscape (MIEL) analysis to characterize HIV ARV effects on hNPC epigenetic signature. To test for ARV effects on neurogenesis, we treated hNPCs with 0.1,1.0, or 10 µM of each ARV for three days. After treatment with 0.1, 1.0, or 10 µM

bioRxiv preprint doi: https://doi.org/10.1101/2020.09.05.284422; this version posted January 11, 2021. The copyright holder for this preprint (which was not certified by peer review) is the author/funder, who has granted bioRxiv a license to display the preprint in perpetuity. It is made available under aCC-BY-NC-ND 4.0 International license.

DTG, EVG, or FTC, hNPC viability was similar to DMSO controls. Treatment with 10 µM TDF, however, significantly reduced hNPC viability by 30% (Fig. 7A). hNPC viability was also reduced by 3 µM SAHA (45%), a histone deacetylase inhibitor, and by 10 µM GSK343 (50%), a histone methyltransferase inhibitor. hNPC viability was not affected by 0.3 µM JQ1, which inhibits the interaction of bromodomain-containing proteins with acetylated histones, or by 1 µM tofacitinib, which inhibits JAK activity.

To analyze ARV effects on hNPC epigenetics, we immunolabeled hNPCs for two sets of histone modifications: H3K27me3 (condensed chromatin) and H3K27ac (active enhancers) or H3K9me3 (condensed chromatin) and H3K4me1 (primed enhancers). We then scanned the cells using Vala's IC200 Image Cytometer and analyzed the images to identify the multivariate epigenetic signatures of each histone modification in each condition. We characterized the epigenetic signatures using texture features[56,65,66] rather than intensities and morphologies to reduce culturing and immunolabeling artifacts. Quadratic discriminant analysis reports changes in the epigenetic signatures in response to each treatment. SAHA and GSK43, which decreased hNPC viability, also significantly affected the H3K27me3/H3K27ac (Fig. 7B) and the H3K9me3/H3K4me1 (Fig. 7C) epigenetic signatures, with discriminant analysis separating samples treated with these compounds from DMSO- and ARV-treated samples. Of the ARVs tested, only 10 µM TDF altered the epigenetic signature, with TDF-treated samples clustering together and separately from DMSO-, SAHA-, and GSK343-treated samples in both H3K27me3/H3K27ac and H3K9me3/HeK4me1 plots (Fig. 7B, C).

Confusion matrices report the ability of the multiparametric discriminant analysis to correctly classify each sample with other samples that received the same treatment compared to other treatments (Fig. 7D, E)[56]. The confusion matrix for both H3K27me3/H3K27ac and H3K9me3/H3K4me1 show that classification occurred correctly 100% of the time for samples treated with 10 µM GSK343, 3 µM SAHA, and 10 µM TDF. This classification accuracy supports

bioRxiv preprint doi: https://doi.org/10.1101/2020.09.05.284422; this version posted January 11, 2021. The copyright holder for this preprint (which was not certified by peer review) is the author/funder, who has granted bioRxiv a license to display the preprint in perpetuity. It is made available under aCC-BY-NC-ND 4.0 International license.

our conclusion that these three compounds are epigenotoxic and significantly alter the hNPC epigenetic landscape. Samples treated with DMSO, DTG, EVG, FTC, JQ1, or TOF, which clustered together after discriminant analysis, were correctly classified less than 100% of the time.

The results from the MIEL assay demonstrate that TDF, but not DTG, EVG, or FTC, reduced viability and altered the pattern of the H3K27me3, H3K27ac, H3K9me3, and H3K4me1 epigenetic histone modifications in hNPCs.

bioRxiv preprint doi: https://doi.org/10.1101/2020.09.05.284422; this version posted January 11, 2021. The copyright holder for this preprint (which was not certified by peer review) is the author/funder, who has granted bioRxiv a license to display the preprint in perpetuity. It is made available under aCC-BY-NC-ND 4.0 International license.

Discussion

In this study, we developed HCA and KIC methods to quantify neurotoxic and neurodevelopmental effects of HIV ARVs in hiPSC-neurons and human neural precursor cells (Fig. 8). Loss of function and/or cell death in excitatory neurons resulting from ARV neurotoxicity could contribute to HIV-associated neurocognitive disorders (HAND), which currently affect about half of people with HIV[17,18]. Because people with HIV develop non-AIDs-related health conditions, including cognitive decline, at an earlier age than the general population[67-69], HAND is likely to increase in incidence and severity as the percentage of people with HIV over 50 years old increases[70]. ARV exposure during fetal development, childhood, and adolescence may also increase HAND incidence by affecting neurogenesis at key stages in CNS development. Human in vitro systems are needed to identify and mitigate ARV neurotoxicity and neurodevelopmental effects. The methods used in this study feature automated digital microscopy and analysis for cell plated in 384-well dishes, a format that facilitates higher throughput testing of ARVs at multiple concentrations and combinations, as well as testing of potential HAND therapeutics that may mitigate ARV neurotoxicity.

Many previous in vitro studies of ARV neurotoxicity have been conducted with primary embryonic rat neurons. Exposure of these cells to 10 µM of the integrase inhibitor EVG for four days, but not two days, significantly reduced the number of MAP2+ neurons[28], while 0.1 and 1 µM EVG were not neurotoxic. In this study, we found that seven-day exposure (but not one-day exposure) to 10 µM EVG reduced hiPSC-neuron viability, decreased neurite length and synapse density, and inhibited intracellular calcium transients, confirming the neurotoxicity of this compound in a human neuron model. We also observed milder toxic effects after treatment with 10 µM of the integrase inhibitor DTG and 10 µM of the nucleoside/nucleotide reverse transcriptase inhibitor TDF. The nucleoside/nucleotide reverse transcriptase inhibitor FTC, which forms a base

bioRxiv preprint doi: https://doi.org/10.1101/2020.09.05.284422; this version posted January 11, 2021. The copyright holder for this preprint (which was not certified by peer review) is the author/funder, who has granted bioRxiv a license to display the preprint in perpetuity. It is made available under aCC-BY-NC-ND 4.0 International license.

for front-line recommended cART regimens in the US, was relatively non-toxic in our hiPSC-neuron model.

Our data suggest that plasma, CSF, and brain concentrations of DTG, EVG, and TDF need to be managed to control HIV replication while minimizing ARV neurotoxicity. Efforts to increase the CNS penetration effectiveness (CPE) of ARVs such as EVG[71] and protease inhibitors[72] may decrease the CNS viral load but may also increase ARV neurotoxicity. Neuroimaging studies have shown that HAND patients on cART have locally compromised blood brain barriers[73], which could increase ARV levels in the brain, even for ARVs with low CPE scores. In postmortem brains from HIV-positive people who died while on cART, higher ARV levels were associated with worse antemortem cognitive performance[74]. This association could result from HIV-induced systemic inflammation that leads to blood brain barrier compromise or from increased ARV neurotoxicity. Our human in vitro assays enable direct testing of ARVs for neurotoxicity, which is likely to be relevant to HAND pathology.

While our assay used hiPSC-neurons in isolation, neurons coexist with glial cells like microglia and astrocytes in vivo, which impact their survival and function[75] and play key roles in neuroinflammation and neurodegenerative diseases such as Alzheimer's[76,77]. A recently developed in vitro model enables testing for ARV neurotoxicity on co-cultured hiPSC-neurons, -microglia, and -astrocytes[78] in the presence or absence of HIV infection. In this system, efavirenz, a nucleoside/nucleotide reverse transcriptase inhibitor linked to neuropsychiatric and cognitive effects[79-81], increased inflammation and reduced phagocytosis in the hiPSC-microglia. Our hiPSC-neuron assay could be similarly expanded to include hiPSC-microglia and -astrocytes to test whether glia contribute to or protect against ARV-induced neuronal toxicity. This expanded system will also enable testing of the efficacy of ARVs to inhibit HIV infection of human microglia and the resulting inflammation[82,83].

bioRxiv preprint doi: https://doi.org/10.1101/2020.09.05.284422; this version posted January 11, 2021. The copyright holder for this preprint (which was not certified by peer review) is the author/funder, who has granted bioRxiv a license to display the preprint in perpetuity. It is made available under aCC-BY-NC-ND 4.0 International license.

Our assay of ARV effects in hNPCs indicated that TDF reduces viability in this cell type. TDF and zidovidine (AZT) reduce the viability of murine NPCs[84,85], but to our knowledge this is the first report of ARV effects on human NPCs. TDF also altered the distribution of histone modifications in hNPCs, which may indicate that TDF affects hNPC differentiation. Because ARVs are prescribed as combinations of several drugs, it will be important to investigate such combinations for their epigenotoxic activity. DNA methylation, another epigenetic modification, has recently been reported to be altered in HIV+ children receiving cART[86]. Given the importance of neurogenesis in neurodevelopment and maintenance of cognitive function during aging, it is critical to evaluate existing and candidate ARVs for effects on hNPC viability and epigenetics.

In summary, we have developed and applied methods for the high throughput testing of HIV ARVs on hiPSC-neurons that model excitatory neurons of the human brain. Similar HCA and KIC methods have been applied to quantify neurotoxic effects of the breast cancer therapeutic tamoxifen in primary rat hippocampal neurons[50], suggesting a broad applicability for these methods for neurotoxicity screening. We have also developed methods to screen for ARV effects on neurogenesis by quantifying the viability and epigenetics of hNPCs. Developing cART regimens that balance the neuroprotective effects of suppressing CNS HIV replication with potential ARV neurotoxicity remains a major challenge in HIV/AIDS treatment and drug discovery[87-89]. The results of the present study represent progress in this direction. Future studies will incorporate human glial cells (hiPSC-microglia and hiPSC-astrocytes) into our assay system to increase its power to detect neurotoxic and neurodevelopmental effects of existing and candidate anti-HIV therapeutics and to identify potential HAND therapeutics that can mitigate these effects.

bioRxiv preprint doi: https://doi.org/10.1101/2020.09.05.284422; this version posted January 11, 2021. The copyright holder for this preprint (which was not certified by peer review) is the author/funder, who has granted bioRxiv a license to display the preprint in perpetuity. It is made available under aCC-BY-NC-ND 4.0 International license.

Acknowledgements:

This study was funded, in part, by grants from the NIH, which include R44ES026268 “Assay of chemicals for Parkinson's toxicity in human iPSC-derived neurons” and R41MH119621 “The Microscopic Imaging of Epigenetic Landscape- NeuroDevelopment (MIEL-ND) assay” and 1R43AG062012-01 “The Alzheimer's Therapeutics Screening Assay: a high-throughput drug-discovery platform utilizing neurons and microglia derived from human induced pluripotent stem cells and Kinetic Image Cytometry”.

bioRxiv preprint doi: https://doi.org/10.1101/2020.09.05.284422; this version posted January 11, 2021. The copyright holder for this preprint (which was not certified by peer review) is the author/funder, who has granted bioRxiv a license to display the preprint in perpetuity. It is made available under aCC-BY-NC-ND 4.0 International license.

Figure Legends

Figure 1. Single ARVs decrease viability and neurite length in hiPSC-neurons in a dose-dependent manner. hiPSC-neurons were exposed to the ARVs for 7 days. (A) Representative images of hiPSC-neurons treated with DMSO alone or 10 µM dolutegravir (DTG), elvitegravir (EVG), tenofovir disproxil fumarate (TDF), or emtricitabine (FTC), fixed, and stained for nuclei (Hoechst, blue) and neuronal somas and neurites (Tuj-1, grayscale). Scale bar = 50 µm. (B-D) Viability and neurite data for hiPSC-neurons treated with DMSO alone, ARVs (0.1, 1, or 10 µM) or blebbistatin (25 µM). (B) Neuronal viability as defined by the number of live neuron nuclei in each well relative to the DMSO control mean. (C) Total neurite length in µm per cm^2 image area for each condition. (D) Total neurite length per live neuron nucleus for each condition. Each dot represents the average of each measurement from nine images per well. DMSO and blebbistatin: n = 18 wells; ARVs: n = 6 wells. Bars represent mean ± standard deviation. Statistics performed with one-way ANOVA followed by Dunnett's multiple comparisons test. * $p < 0.05$, ** $p < 0.01$, *** $p < 0.001$.

Figure 2. Single and combined ARVs decrease viability and neurite length in hiPSC-neurons after seven days, but not one day of exposure. hiPSC-neurons were treated for one (left) or seven days (right) with DMSO alone, 25 µM blebbistatin, single ARVs, or combinations of ARVs (each at 10 µM). (A, D) Neuronal viability as defined by the number of live neuron nuclei in each well relative to the DMSO control mean. (B, E) Total neurite length in µm per cm^2 image area in each well relative to the DMSO control mean. (C, F) Total neurite length per live neuron nucleus in each well relative to the DMSO control mean. Each dot represents the average of each measurement from nine images per well. One-day treatment DMSO and blebbistatin: n = 18 wells;

bioRxiv preprint doi: https://doi.org/10.1101/2020.09.05.284422; this version posted January 11, 2021. The copyright holder for this preprint (which was not certified by peer review) is the author/funder, who has granted bioRxiv a license to display the preprint in perpetuity. It is made available under aCC-BY-NC-ND 4.0 International license.

ARVs: n = 6 wells. Seven-day treatment DMSO and blebbistatin: n = 36 wells; ARVs: n = 12 wells from two experiments. Bars represent mean ± standard deviation. Statistics performed with one-way ANOVA followed by Tukey's multiple comparisons test. * $p < 0.05$, ** $p < 0.01$, *** $p < 0.001$. Significant differences between DMSO and ARV or blebbistatin treatments are indicated on each graph. Significant differences between DTG and other ARVs/combinations are indicated with "a", significant differences between EVG and other ARVs/combinations are indicated with "b", and significant differences between TDF and other ARVs/combinations are indicated with "c". Results of other Tukey's comparisons are reported in Figures S1-S3.

Figure 3. Single ARVs affect synapse density in hiPSC-neurons in a dose-dependent manner. (A) Representative images of hiPSC-neurons from the same experiment in Figure 1 (seven-day ARV treatment) stained for SV2 (presynaptic marker, left) and PSD95 (postsynaptic marker, center). Right images show live neuron nuclei (green), neurites (cyan), and synapses (magenta) identified by CyteSeer. Scale bar = 50 µm. (B) Synapse Density (synapses per cm^2 imaging area) for each condition. (C) Synapses/Neurite Length (synapses per µm neurite length) for each condition. Each dot represents the average of each measurement from nine images per well. DMSO and blebbistatin: n = 18 wells; ARVs: n = 6 wells. Bars represent mean ± standard deviation. Statistics performed with one-way ANOVA followed by Dunnett's multiple comparisons test. * $p < 0.05$, ** $p < 0.01$, *** $p < 0.001$.

Figure 4. Single and combined ARVs affect synapse density of hiPSC-neurons after seven days, but not one day of exposure. hiPSC-neurons were treated for one or seven days with DMSO alone, 25 µM blebbistatin, single ARVs, or combinations of ARVs (each at 10 µM). (A, C) Synapse Density (synapses per cm^2 image area) in each well relative to the DMSO control mean.

bioRxiv preprint doi: https://doi.org/10.1101/2020.09.05.284422; this version posted January 11, 2021. The copyright holder for this preprint (which was not certified by peer review) is the author/funder, who has granted bioRxiv a license to display the preprint in perpetuity. It is made available under aCC-BY-NC-ND 4.0 International license.

(B, D) Synapses/Neurite Length (synapses per µm neurite length) in each well relative to the DMSO control mean. Each dot represents the average of each measurement from nine images per well. One day treatment DMSO and blebbistatin: n = 18 wells; ARVs: n = 6 wells. Seven day treatment DMSO and blebbistatin: n = 36 wells; ARVs: n = 12 wells from two experiments. Bars represent mean ± standard deviation. Statistics performed with one-way ANOVA followed by Tukey's multiple comparisons test. * $p < 0.05$, ** $p < 0.01$, *** $p < 0.001$. Significant differences between DMSO and ARV or blebbistatin treatments are indicated on each graph. Significant differences between DTG and other ARVs/combinations are indicated with "a", significant differences between EVG and other ARVs/combinations are indicated with "b", and significant differences between TDF and other ARVs/combinations are indicated with "c". Results of other Tukey's comparisons are reported in Figures S4 and S5.

Figure 5. Effect of ARVs on calcium transients in hiPSC-neurons. hiPSC-neurons were treated for seven days with DMSO alone, single ARVs, or combinations of ARVs (each at 10 µM). (A-H) Traces showing transient increases in calcium fluorescence relative to baseline. Each graph contains one trace for each active neuron in each condition with detectable increases in calcium fluorescence. DMSO: 1034 cells; DTG: 716 cells; EVG: 31 cells; TDF: 729 cells; FTC: 1003 cells; DTG/TDF/FTC: 134 cells; EVG/TDF/FTC: 17 cells; TDF/FTC: 539 cells. Six wells per condition.

Figure 6. Quantification of the effects of ARVs on calcium activity in hiPSC-neurons. hiPSC-neurons were treated for one or seven days with DMSO alone, single ARVs, or combinations of ARVs (each at 10 µM). (A, D) Percent of live neurons that are active with detectable calcium transients in each condition. (B, E) The mean event frequency of calcium transients of all active neurons in each well. (C, F) The mean of mean calcium peak amplitudes

bioRxiv preprint doi: https://doi.org/10.1101/2020.09.05.284422; this version posted January 11, 2021. The copyright holder for this preprint (which was not certified by peer review) is the author/funder, who has granted bioRxiv a license to display the preprint in perpetuity. It is made available under aCC-BY-NC-ND 4.0 International license.

of all active neurons in each well. Six wells per condition. Bars represent mean ± standard deviation. Statistics performed with one-way ANOVA followed by Tukey's multiple comparisons test. * $p < 0.05$, ** $p < 0.01$, *** $p < 0.001$ vs. DMSO. Significant differences between DTG and other ARVs/combinations are indicated with "a", significant differences between EVG and other ARVs/combinations are indicated with "b", and significant differences between TDF and other ARVs/combinations are indicated with "c". Results of other Tukey's comparisons are reported in Figures S6-S8.

Figure 7. TDF affects the viability and epigenetic signature of hNPCs. Fetal hNPCs were treated with DMSO alone, compounds with known epigenetic effects (SAHA, GSK343, JQ1, or TOF), or ARVs at the indicated concentrations. (A) Count of hNPCs per well for each condition following treatment. Bars represent mean ± standard deviation. Statistics performed with one-way ANOVA followed by Dunnett's multiple comparisons test. * $p < 0.05$. (B-E) Quadratic discriminant analysis using texture features derived from images of hNPCs treated with the indicated compounds and immunostained for H3K27me3 and H3K27ac (B, D) or H3K9me3 and H3K4me1 (C, E). (B, C) Scatter plots showing the first two texture-derived discriminant factors for each condition. (D, E) Confusion matrices showing the results of the discriminant analysis. Numbers represent the percent of wells classified correctly (on the diagonal) and incorrectly (off the diagonal). N = 6 wells per condition.

Figure 8. HCA, KIC, and MIEL to identify diverse neurotoxic effects of HIV antiretrovirals. (Top) Outline of our methods to identify HIV antiretroviral effects in hiPSC-neurons. After culture in imaging-quality 384-well plates, hiPSC-neurons are exposed to ARVs alone or in combination for one or seven days. hiPSC-neurons are then fixed and stained for high content analysis or

bioRxiv preprint doi: https://doi.org/10.1101/2020.09.05.284422; this version posted January 11, 2021. The copyright holder for this preprint (which was not certified by peer review) is the author/funder, who has granted bioRxiv a license to display the preprint in perpetuity. It is made available under aCC-BY-NC-ND 4.0 International license.

imaged live for KIC of intracellular calcium transients. These assays test if ARVs alter hiPSC-neuron viability, neurite length, synapse density, and/or calcium transient activity. (Bottom) Outline of our methods to identify ARV effects in hNPCs. After culture in imaging-quality 384-well plates, hNPCs are exposed to ARVs for three days. hNPCs are then fixed and stained for microscopic imaging of the epigenetic landscape (MIEL) analysis. This assay tests if ARVs affect hNPC viability and/or change the histone modification pattern within the nuclei. Figure made with Biorender.com.

Table S1. Tukey's multiple comparison test results for Neuronal Viability. Tables show the results of each pairwise comparison for hiPSC-neurons treated for one (left) or seven days (right) with DMSO alone, 25 µM blebbistatin, single ARVs, or combinations of ARVs (each at 10 µM). See Figure 2A, D for graph of results. ns: not significant ($p > 0.05$) * $p < 0.05$, ** $p < 0.01$, *** $p < 0.001$.

Table S2. Tukey's multiple comparison test results for Total Neurite Length. Tables show the results of each pairwise comparison for hiPSC-neurons treated for one (left) or seven days (right) with DMSO alone, 25 µM blebbistatin, single ARVs, or combinations of ARVs (each at 10 µM). See Figure 2B, E for graph of results. ns: not significant ($p > 0.05$) * $p < 0.05$, ** $p < 0.01$, *** $p < 0.001$.

Table S3. Tukey's multiple comparison test results for Neurite Length per Neuron. Tables show the results of each pairwise comparison for hiPSC-neurons treated for one (left) or seven days (right) with DMSO alone, 25 µM blebbistatin, single ARVs, or combinations of ARVs (each

bioRxiv preprint doi: https://doi.org/10.1101/2020.09.05.284422; this version posted January 11, 2021. The copyright holder for this preprint (which was not certified by peer review) is the author/funder, who has granted bioRxiv a license to display the preprint in perpetuity. It is made available under aCC-BY-NC-ND 4.0 International license.

at 10 µM). See Figure 2C, F for graph of results. ns: not significant ($p > 0.05$) * $p < 0.05$, ** $p < 0.01$, *** $p < 0.001$.

Table S4. Tukey's multiple comparison test results for Synapse Density. Tables show the results of each pairwise comparison for hiPSC-neurons treated for one (left) or seven days (right) with DMSO alone, 25 µM blebbistatin, single ARVs, or combinations of ARVs (each at 10 µM). See Figure 4A, C for graph of results. ns: not significant ($p > 0.05$) * $p < 0.05$, ** $p < 0.01$, *** $p < 0.001$.

Table S5. Tukey's multiple comparison test results for Synapses/Neurite Length. Tables show the results of each pairwise comparison for hiPSC-neurons treated for one (left) or seven days (right) with DMSO alone, 25 µM blebbistatin, single ARVs, or combinations of ARVs (each at 10 µM). See Figure 4B, D for graph of results. ns: not significant ($p > 0.05$) * $p < 0.05$, ** $p < 0.01$, *** $p < 0.001$.

Table S6. Tukey's multiple comparison test results for percent neurons with calcium transient activity. Tables show the results of each pairwise comparison for hiPSC-neurons treated for one (left) or seven days (right) with DMSO alone, single ARVs, or combinations of ARVs (each at 10 µM). See Figure 6A, D for graph of results. ns: not significant ($p > 0.05$) * $p < 0.05$, ** $p < 0.01$, *** $p < 0.001$.

Table S7. Tukey's multiple comparison test results for calcium transient event frequency. Tables show the results of each pairwise comparison for hiPSC-neurons treated for one (left) or

bioRxiv preprint doi: https://doi.org/10.1101/2020.09.05.284422; this version posted January 11, 2021. The copyright holder for this preprint (which was not certified by peer review) is the author/funder, who has granted bioRxiv a license to display the preprint in perpetuity. It is made available under aCC-BY-NC-ND 4.0 International license.

seven days (right) with DMSO alone, single ARVs, or combinations of ARVs (each at 10 µM). See Figure 6B, E for graph of results. ns: not significant ($p > 0.05$) * $p < 0.05$, ** $p < 0.01$, *** $p < 0.001$.

Table S8. Tukey's multiple comparison test results for calcium transient mean peak amplitude. Tables show the results of each pairwise comparison for hiPSC-neurons treated for one (left) or seven days (right) with DMSO alone, single ARVs, or combinations of ARVs (each at 10 µM). See Figure 6C, F for graph of results. ns: not significant ($p > 0.05$) * $p < 0.05$, ** $p < 0.01$, *** $p < 0.001$.

bioRxiv preprint doi: https://doi.org/10.1101/2020.09.05.284422; this version posted January 11, 2021. The copyright holder for this preprint (which was not certified by peer review) is the author/funder, who has granted bioRxiv a license to display the preprint in perpetuity. It is made available under aCC-BY-NC-ND 4.0 International license.

References

1. Global HIV & AIDS statistics - 2019 fact sheet. Vol. 2020 (UNAIDS).
2. FDA. Attacking AIDS with a 'Cocktail' Therapy: Drug Combo Sends Deaths Plummeting. in *HIV/AIDS News* (1999).
3. Antiretroviral Therapy Cohort, C. Survival of HIV-positive patients starting antiretroviral therapy between 1996 and 2013: a collaborative analysis of cohort studies. *Lancet HIV* **4**, e349-e356 (2017).
4. Cohen, M.S.*, et al.* Antiretroviral Therapy for the Prevention of HIV-1 Transmission. *N Engl J Med* **375**, 830-839 (2016).
5. Rodger, A.J.*, et al.* Sexual Activity Without Condoms and Risk of HIV Transmission in Serodifferent Couples When the HIV-Positive Partner Is Using Suppressive Antiretroviral Therapy. *JAMA* **316**, 171-181 (2016).
6. Grant, R.M.*, et al.* Preexposure chemoprophylaxis for HIV prevention in men who have sex with men. *N Engl J Med* **363**, 2587-2599 (2010).
7. Baeten, J.M.*, et al.* Antiretroviral prophylaxis for HIV prevention in heterosexual men and women. *N Engl J Med* **367**, 399-410 (2012).
8. Choopanya, K.*, et al.* Antiretroviral prophylaxis for HIV infection in injecting drug users in Bangkok, Thailand (the Bangkok Tenofovir Study): a randomised, double-blind, placebo-controlled phase 3 trial. *Lancet* **381**, 2083-2090 (2013).
9. Hurst, S.A., Appelgren, K.E. & Kourtis, A.P. Prevention of mother-to-child transmission of HIV type 1: the role of neonatal and infant prophylaxis. *Expert Rev Anti Infect Ther* **13**, 169-181 (2015).
10. McCormack, S.A. & Best, B.M. Protecting the fetus against HIV infection: a systematic review of placental transfer of antiretrovirals. *Clin Pharmacokinet* **53**, 989-1004 (2014).
11. Sacktor, N. The epidemiology of human immunodeficiency virus-associated neurological disease in the era of highly active antiretroviral therapy. *J Neurovirol* **8 Suppl 2**, 115-121 (2002).
12. Sacktor, N.*, et al.* HIV-associated neurologic disease incidence changes:: Multicenter AIDS Cohort Study, 1990-1998. *Neurology* **56**, 257-260 (2001).
13. d'Arminio Monforte, A.*, et al.* Changing incidence of central nervous system diseases in the EuroSIDA cohort. *Ann Neurol* **55**, 320-328 (2004).
14. Committee, U.K.C.H.C.S.S.*, et al.* HIV-associated central nervous system diseases in the recent combination antiretroviral therapy era. *Eur J Neurol* **18**, 527-534 (2011).
15. Heaton, R.K.*, et al.* HIV-associated neurocognitive disorders persist in the era of potent antiretroviral therapy: CHARTER Study. *Neurology* **75**, 2087-2096 (2010).
16. Cysique, L.A., Maruff, P. & Brew, B.J. Prevalence and pattern of neuropsychological impairment in human immunodeficiency virus-infected/acquired immunodeficiency syndrome (HIV/AIDS) patients across pre- and post-highly active antiretroviral therapy eras: a combined study of two cohorts. *J Neurovirol* **10**, 350-357 (2004).
17. Smail, R.C. & Brew, B.J. HIV-associated neurocognitive disorder. *Handb Clin Neurol* **152**, 75-97 (2018).
18. Saylor, D.*, et al.* HIV-associated neurocognitive disorder - pathogenesis and prospects for treatment. *Nat Rev Neurol* **12**, 309 (2016).
19. Heaton, R.K.*, et al.* Neuropsychological impairment in human immunodeficiency virus-infection: implications for employment. HNRC Group. HIV Neurobehavioral Research Center. *Psychosom Med* **56**, 8-17 (1994).
20. Brew, B.J. Benefit or toxicity from neurologically targeted antiretroviral therapy? *Clin Infect Dis* **50**, 930-932 (2010).

bioRxiv preprint doi: https://doi.org/10.1101/2020.09.05.284422; this version posted January 11, 2021. The copyright holder for this preprint (which was not certified by peer review) is the author/funder, who has granted bioRxiv a license to display the preprint in perpetuity. It is made available under aCC-BY-NC-ND 4.0 International license.

21. Gorman, A.A., Foley, J.M., Ettenhofer, M.L., Hinkin, C.H. & van Gorp, W.G. Functional consequences of HIV-associated neuropsychological impairment. *Neuropsychol Rev* **19**, 186-203 (2009).
22. Grant, I.*, et al.* Asymptomatic HIV-associated neurocognitive impairment increases risk for symptomatic decline. *Neurology* **82**, 2055-2062 (2014).
23. Heaton, R.K.*, et al.* Neurocognitive change in the era of HIV combination antiretroviral therapy: the longitudinal CHARTER study. *Clin Infect Dis* **60**, 473-480 (2015).
24. Underwood, J., Robertson, K.R. & Winston, A. Could antiretroviral neurotoxicity play a role in the pathogenesis of cognitive impairment in treated HIV disease? *AIDS* **29**, 253-261 (2015).
25. Akay, C.*, et al.* Antiretroviral drugs induce oxidative stress and neuronal damage in the central nervous system. *J Neurovirol* **20**, 39-53 (2014).
26. Robertson, K., Liner, J. & Meeker, R.B. Antiretroviral neurotoxicity. *J Neurovirol* **18**, 388-399 (2012).
27. Zhang, Y.*, et al.* Long-term exposure of mice to nucleoside analogues disrupts mitochondrial DNA maintenance in cortical neurons. *PLoS One* **9**, e85637 (2014).
28. Stern, A.L.*, et al.* Differential Effects of Antiretroviral Drugs on Neurons In Vitro: Roles for Oxidative Stress and Integrated Stress Response. *J Neuroimmune Pharmacol* **13**, 64-76 (2018).
29. Schweinsburg, B.C.*, et al.* Brain mitochondrial injury in human immunodeficiency virus-seropositive (HIV+) individuals taking nucleoside reverse transcriptase inhibitors. *J Neurovirol* **11**, 356-364 (2005).
30. Jernigan, T.L.*, et al.* Clinical factors related to brain structure in HIV: the CHARTER study. *J Neurovirol* **17**, 248-257 (2011).
31. Jensen, B.K.*, et al.* Altered Oligodendrocyte Maturation and Myelin Maintenance: The Role of Antiretrovirals in HIV-Associated Neurocognitive Disorders. *J Neuropathol Exp Neurol* **74**, 1093-1118 (2015).
32. Chang, L., Yakupov, R., Nakama, H., Stokes, B. & Ernst, T. Antiretroviral treatment is associated with increased attentional load-dependent brain activation in HIV patients. *J Neuroimmune Pharmacol* **3**, 95-104 (2008).
33. Tozzi, V.*, et al.* Changes in cognition during antiretroviral therapy: comparison of 2 different ranking systems to measure antiretroviral drug efficacy on HIV-associated neurocognitive disorders. *J Acquir Immune Defic Syndr* **52**, 56-63 (2009).
34. Santos, G.M.A.*, et al.* Cross-Sectional and Cumulative Longitudinal Central Nervous System Penetration Effectiveness Scores Are Not Associated With Neurocognitive Impairment in a Well Treated Aging Human Immunodeficiency Virus-Positive Population in Switzerland. *Open Forum Infect Dis* **6**, ofz277 (2019).
35. Marra, C.M.*, et al.* Impact of combination antiretroviral therapy on cerebrospinal fluid HIV RNA and neurocognitive performance. *AIDS* **23**, 1359-1366 (2009).
36. Kahouadji, Y.*, et al.* Cognitive function after several years of antiretroviral therapy with stable central nervous system penetration score. *HIV Med* **14**, 311-315 (2013).
37. Caniglia, E.C.*, et al.* Antiretroviral penetration into the CNS and incidence of AIDS-defining neurologic conditions. *Neurology* **83**, 134-141 (2014).
38. Robertson, K.R.*, et al.* Neurocognitive effects of treatment interruption in stable HIV-positive patients in an observational cohort. *Neurology* **74**, 1260-1266 (2010).
39. Dahabieh, M.S., Battivelli, E. & Verdin, E. Understanding HIV latency: the road to an HIV cure. *Annu Rev Med* **66**, 407-421 (2015).
40. Siliciano, R.F. & Greene, W.C. HIV latency. *Cold Spring Harb Perspect Med* **1**, a007096 (2011).
41. Cohen, S.*, et al.* Poorer cognitive performance in perinatally HIV-infected children versus healthy socioeconomically matched controls. *Clin Infect Dis* **60**, 1111-1119 (2015).

bioRxiv preprint doi: https://doi.org/10.1101/2020.09.05.284422; this version posted January 11, 2021. The copyright holder for this preprint (which was not certified by peer review) is the author/funder, who has granted bioRxiv a license to display the preprint in perpetuity. It is made available under aCC-BY-NC-ND 4.0 International license.

42. Van den Hof, M.*, et al.* Lower IQ and poorer cognitive profiles in treated perinatally HIV-infected children is irrespective of having a background of international adoption. *PLoS One* **14**, e0224930 (2019).
43. Crowell, C.S., Malee, K.M., Yogev, R. & Muller, W.J. Neurologic disease in HIV-infected children and the impact of combination antiretroviral therapy. *Rev Med Virol* **24**, 316-331 (2014).
44. Sherr, L., Croome, N., Parra Castaneda, K. & Bradshaw, K. A systematic review of psychological functioning of children exposed to HIV: using evidence to plan for tomorrow's HIV needs. *AIDS Behav* **18**, 2059-2074 (2014).
45. Brown, L.A.*, et al.* Efavirenz promotes beta-secretase expression and increased Abeta1-40,42 via oxidative stress and reduced microglial phagocytosis: implications for HIV associated neurocognitive disorders (HAND). *PLoS One* **9**, e95500 (2014).
46. Gannon, P.J.*, et al.* HIV Protease Inhibitors Alter Amyloid Precursor Protein Processing via beta-Site Amyloid Precursor Protein Cleaving Enzyme-1 Translational Up-Regulation. *Am J Pathol* **187**, 91-109 (2017).
47. Giunta, B.*, et al.* Antiretroviral medications disrupt microglial phagocytosis of beta-amyloid and increase its production by neurons: implications for HIV-associated neurocognitive disorders. *Mol Brain* **4**, 23 (2011).
48. Fields, J.A., Swinton, M.K., Soontornniyomkij, B., Carson, A. & Achim, C.L. Beta amyloid levels in cerebrospinal fluid of HIV-infected people vary by exposure to antiretroviral therapy. *AIDS* **34**, 1001-1007 (2020).
49. Xu, J. & Ikezu, T. The comorbidity of HIV-associated neurocognitive disorders and Alzheimer's disease: a foreseeable medical challenge in post-HAART era. *J Neuroimmune Pharmacol* **4**, 200-212 (2009).
50. McDonough, P.M., Prigozhina, N.L., Basa, R.C.B. & Price, J.H. Assay of Calcium Transients and Synapses in Rat Hippocampal Neurons by Kinetic Image Cytometry and High-Content Analysis: An In Vitro Model System for Postchemotherapy Cognitive Impairment. *Assay Drug Dev Technol* **15**, 220-236 (2017).
51. Hunsberger, J.G.*, et al.* Induced Pluripotent Stem Cell Models to Enable In Vitro Models for Screening in the Central Nervous System. *Stem Cells Dev* **24**, 1852-1864 (2015).
52. Miki, D.*, et al.* Characterization of Functional Primary Cilia in Human Induced Pluripotent Stem Cell-Derived Neurons. *Neurochem Res* **44**, 1736-1744 (2019).
53. Sherman, S.P. & Bang, A.G. High-throughput screen for compounds that modulate neurite growth of human induced pluripotent stem cell-derived neurons. *Dis Model Mech* **11**(2018).
54. Urban, N. & Guillemot, F. Neurogenesis in the embryonic and adult brain: same regulators, different roles. *Front Cell Neurosci* **8**, 396 (2014).
55. Hollands, C., Bartolotti, N. & Lazarov, O. Alzheimer's Disease and Hippocampal Adult Neurogenesis; Exploring Shared Mechanisms. *Front Neurosci* **10**, 178 (2016).
56. Farhy, C.*, et al.* Improving drug discovery using image-based multiparametric analysis of the epigenetic landscape. *Elife* **8**(2019).
57. Limouze, J., Straight, A.F., Mitchison, T. & Sellers, J.R. Specificity of blebbistatin, an inhibitor of myosin II. *J Muscle Res Cell Motil* **25**, 337-341 (2004).
58. Straight, A.F.*, et al.* Dissecting temporal and spatial control of cytokinesis with a myosin II Inhibitor. *Science* **299**, 1743-1747 (2003).
59. Davey, S.*, et al.* Mother-to-Child HIV Transmission With In Utero Dolutegravir vs. Efavirenz in Botswana. *J Acquir Immune Defic Syndr* **84**, 235-241 (2020).
60. Smetters, D., Majewska, A. & Yuste, R. Detecting action potentials in neuronal populations with calcium imaging. *Methods* **18**, 215-221 (1999).
61. Rosenberg, S.S. & Spitzer, N.C. Calcium signaling in neuronal development. *Cold Spring Harb Perspect Biol* **3**, a004259 (2011).

bioRxiv preprint doi: https://doi.org/10.1101/2020.09.05.284422; this version posted January 11, 2021. The copyright holder for this preprint (which was not certified by peer review) is the author/funder, who has granted bioRxiv a license to display the preprint in perpetuity. It is made available under aCC-BY-NC-ND 4.0 International license.

62. Fink, C.C. & Meyer, T. Molecular mechanisms of CaMKII activation in neuronal plasticity. *Curr Opin Neurobiol* **12**, 293-299 (2002).
63. Wegierski, T. & Kuznicki, J. Neuronal calcium signaling via store-operated channels in health and disease. *Cell Calcium* **74**, 102-111 (2018).
64. Pfeiffer, E.R., Vega, R., McDonough, P.M., Price, J.H. & Whittaker, R. Specific prediction of clinical QT prolongation by kinetic image cytometry in human stem cell derived cardiomyocytes. *J Pharmacol Toxicol Methods* **81**, 263-273 (2016).
65. Hamilton, N.A., Pantelic, R.S., Hanson, K. & Teasdale, R.D. Fast automated cell phenotype image classification. *BMC Bioinformatics* **8**, 110 (2007).
66. Haralick, R.M., Shanmugam, K. & Dinstein, I. Textural Features for Image Classification. *IEEE Transactions on Systems, Man, and Cybernetics* **SMC-3**, 610-621 (1973).
67. Gross, A.M.*, et al.* Methylome-wide Analysis of Chronic HIV Infection Reveals Five-Year Increase in Biological Age and Epigenetic Targeting of HLA. *Mol Cell* **62**, 157-168 (2016).
68. Nasi, M.*, et al.* Ageing and inflammation in patients with HIV infection. *Clin Exp Immunol* **187**, 44-52 (2017).
69. Shiels, M.S., Pfeiffer, R.M. & Engels, E.A. Age at cancer diagnosis among persons with AIDS in the United States. *Ann Intern Med* **153**, 452-460 (2010).
70. Autenrieth, C.S.*, et al.* Global and regional trends of people living with HIV aged 50 and over: Estimates and projections for 2000-2020. *PLoS One* **13**, e0207005 (2018).
71. Gong, Y.*, et al.* Novel elvitegravir nanoformulation for drug delivery across the blood-brain barrier to achieve HIV-1 suppression in the CNS macrophages. *Scientific reports* **10**, 3835 (2020).
72. Amano, M.*, et al.* Novel Central Nervous System (CNS)-Targeting Protease Inhibitors for Drug-Resistant HIV Infection and HIV-Associated CNS Complications. *Antimicrob Agents Chemother* **63**(2019).
73. Chaganti, J.*, et al.* Imaging correlates of the blood-brain barrier disruption in HIV-associated neurocognitive disorder and therapeutic implications. *AIDS* **33**, 1843-1852 (2019).
74. Ferrara, M.*, et al.* Antiretroviral drug concentrations in brain tissue of adult decedents. *AIDS* **34**, 1907-1914 (2020).
75. Allen, N.J. & Lyons, D.A. Glia as architects of central nervous system formation and function. *Science* **362**, 181-185 (2018).
76. Yang, Q.Q. & Zhou, J.W. Neuroinflammation in the central nervous system: Symphony of glial cells. *Glia* **67**, 1017-1035 (2019).
77. Nirzhor, S.S.R., Khan, R.I. & Neelotpol, S. The Biology of Glial Cells and Their Complex Roles in Alzheimer's Disease: New Opportunities in Therapy. *Biomolecules* **8**(2018).
78. Ryan, S.K.*, et al.* Neuroinflammation and EIF2 Signaling Persist despite Antiretroviral Treatment in an hiPSC Tri-culture Model of HIV Infection. *Stem Cell Reports* **14**, 991 (2020).
79. Apostolova, N.*, et al.* Efavirenz and the CNS: what we already know and questions that need to be answered. *J Antimicrob Chemother* **70**, 2693-2708 (2015).
80. Hakkers, C.S.*, et al.* Objective and Subjective Improvement of Cognition After Discontinuing Efavirenz in Asymptomatic Patients: A Randomized Controlled Trial. *J Acquir Immune Defic Syndr* **80**, e14-e22 (2019).
81. Lapadula, G.*, et al.* Switching from efavirenz to rilpivirine improves sleep quality and self-perceived cognition but has no impact on neurocognitive performances. *AIDS* **34**, 53-61 (2020).
82. Wallet, C.*, et al.* Microglial Cells: The Main HIV-1 Reservoir in the Brain. *Front Cell Infect Microbiol* **9**, 362 (2019).
83. Kaul, M. HIV's double strike at the brain: neuronal toxicity and compromised neurogenesis. *Front Biosci* **13**, 2484-2494 (2008).

bioRxiv preprint doi: https://doi.org/10.1101/2020.09.05.284422; this version posted January 11, 2021. The copyright holder for this preprint (which was not certified by peer review) is the author/funder, who has granted bioRxiv a license to display the preprint in perpetuity. It is made available under aCC-BY-NC-ND 4.0 International license.

84. Xu, P.*, et al.* Combined Medication of Antiretroviral Drugs Tenofovir Disoproxil Fumarate, Emtricitabine, and Raltegravir Reduces Neural Progenitor Cell Proliferation In Vivo and In Vitro. *J Neuroimmune Pharmacol* **12**, 682-692 (2017).
85. Demir, M. & Laywell, E.D. Neurotoxic effects of AZT on developing and adult neurogenesis. *Front Neurosci* **9**, 93 (2015).
86. Shiau, S.*, et al.* Distinct epigenetic profiles in children with perinatally-acquired HIV on antiretroviral therapy. *Sci Rep* **9**, 10495 (2019).
87. Letendre, S. Central nervous system complications in HIV disease: HIV-associated neurocognitive disorder. *Top Antivir Med* **19**, 137-142 (2011).
88. Berger, J.R. & Clifford, D.B. The relationship of CPE to HIV dementia: slain by an ugly fact? *Neurology* **83**, 109-110 (2014).
89. Yuan, N.Y. & Kaul, M. Beneficial and Adverse Effects of cART Affect Neurocognitive Function in HIV-1 Infection: Balancing Viral Suppression against Neuronal Stress and Injury. *J Neuroimmune Pharmacol* (2019).

bioRxiv preprint doi: https://doi.org/10.1101/2020.09.05.284422; this version posted January 11, 2021. The copyright holder for this preprint (which was not certified by peer review) is the author/funder, who has granted bioRxiv a license to display the preprint in perpetuity. It is made available under aCC-BY-NC-ND 4.0 International license.

Table 1. Plasma concentrations of HIV antiretrovirals used in this study.

Antiretroviral	Abbreviation	Drug class	Plasma Cmax
Dolutegravir	DTG	INSTI	8 μM
Elvitegravir	EVG	INSTI	3.5 μM
Tenofovir disproxil fumarate	TDF	NRTI	0.6 μM
Emtricitabine	FTC	NRTI	7 μM

INSTI: integrase strand transfer inhibitor; NRTI: nucleoside/nucleotide reverse transcription inhibitor. Data taken from Food and Drug Administration New Drug Applications for each antiretroviral.

bioRxiv preprint doi: https://doi.org/10.1101/2020.09.05.284422; this version posted January 11, 2021. The copyright holder for this preprint (which was not certified by peer review) is the author/funder, who has granted bioRxiv a license to display the preprint in perpetuity. It is made available under aCC-BY-NC-ND 4.0 International license.

Figure 1

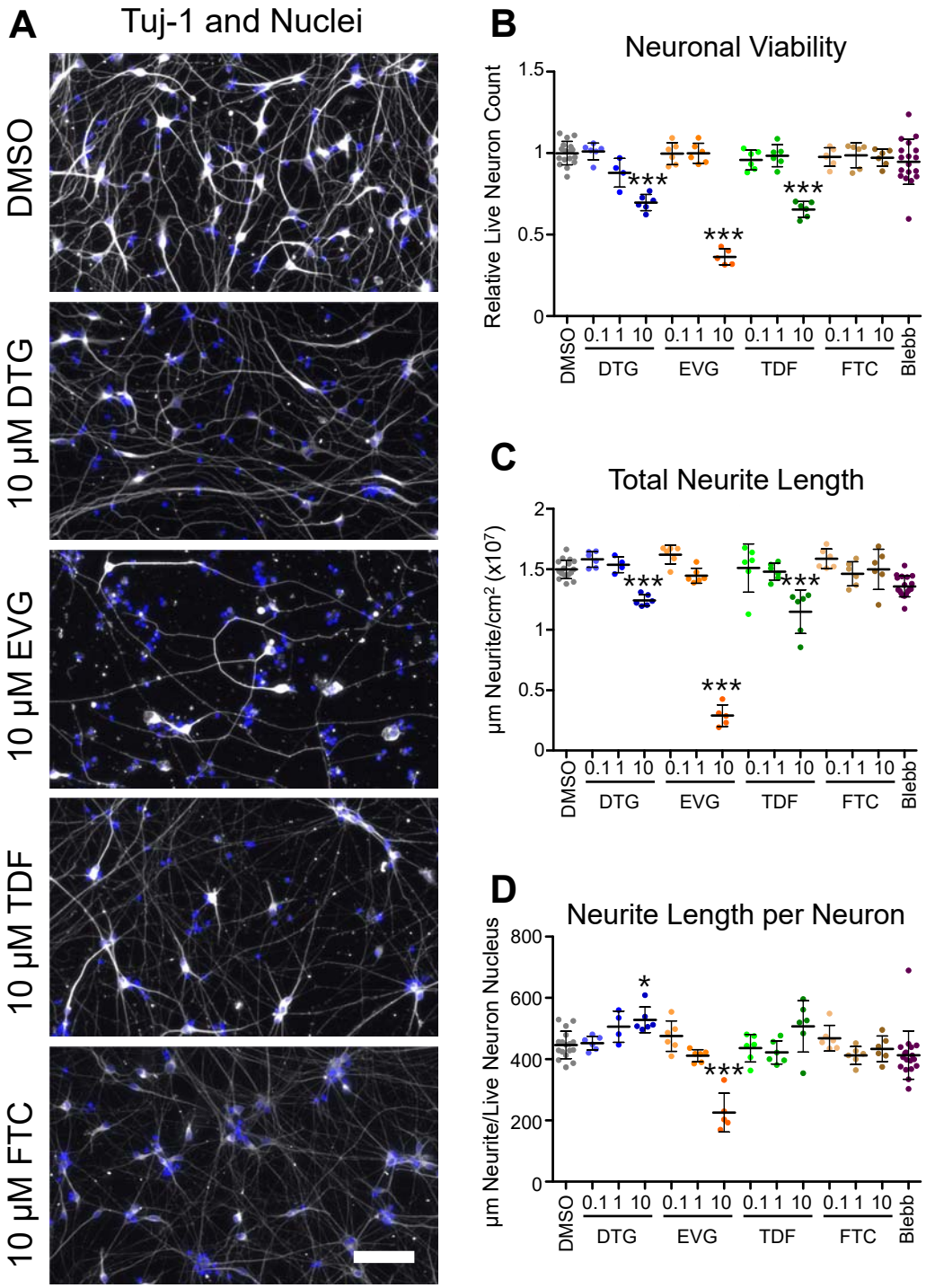

bioRxiv preprint doi: https://doi.org/10.1101/2020.09.05.284422; this version posted January 11, 2021. The copyright holder for this preprint (which was not certified by peer review) is the author/funder, who has granted bioRxiv a license to display the preprint in perpetuity. It is made available under aCC-BY-NC-ND 4.0 International license.

Figure 2

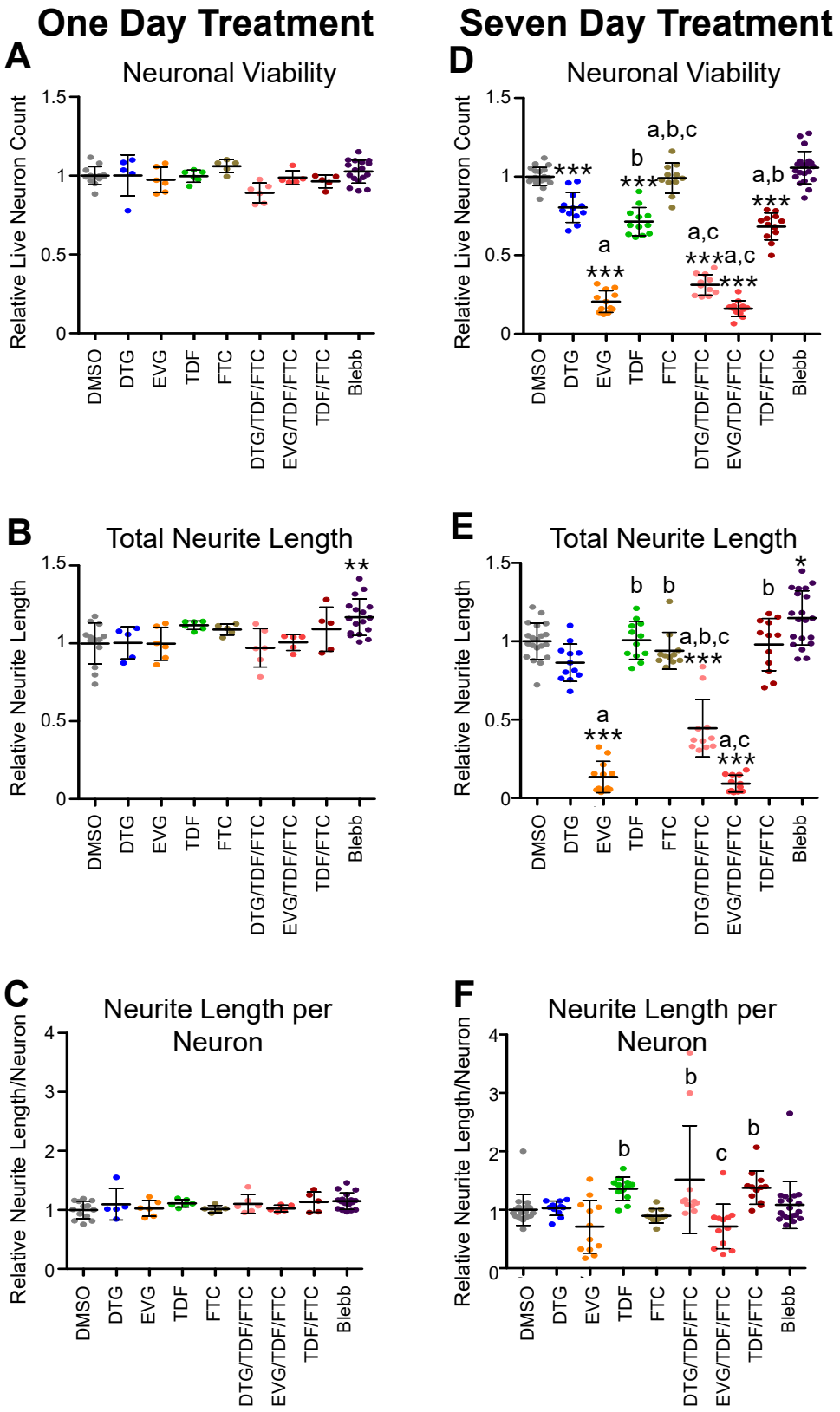

bioRxiv preprint doi: https://doi.org/10.1101/2020.09.05.284422; this version posted January 11, 2021. The copyright holder for this preprint (which was not certified by peer review) is the author/funder, who has granted bioRxiv a license to display the preprint in perpetuity. It is made available under aCC-BY-NC-ND 4.0 International license.

Figure 3

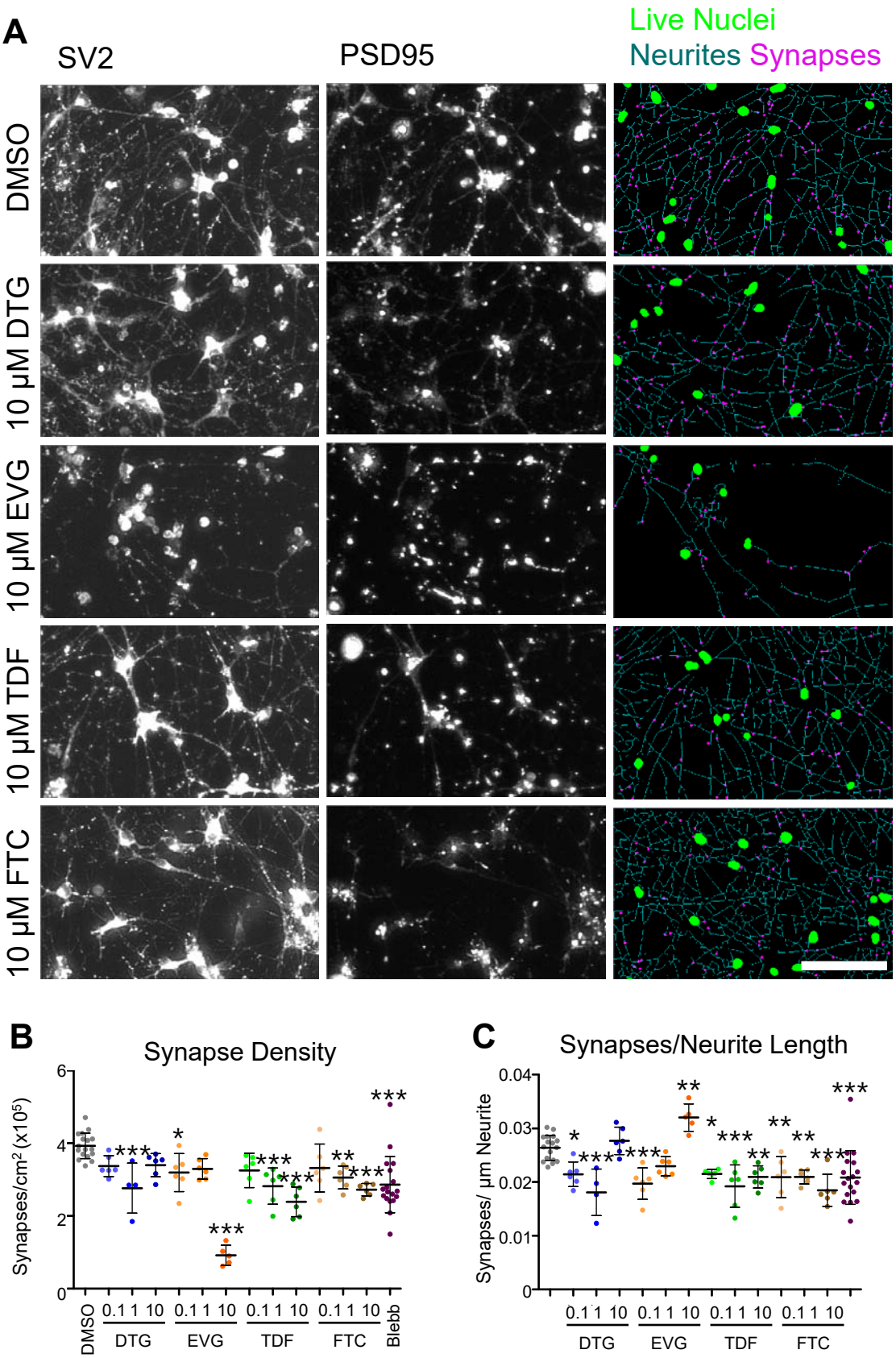

bioRxiv preprint doi: https://doi.org/10.1101/2020.09.05.284422; this version posted January 11, 2021. The copyright holder for this preprint (which was not certified by peer review) is the author/funder, who has granted bioRxiv a license to display the preprint in perpetuity. It is made available under aCC-BY-NC-ND 4.0 International license.

Figure 4

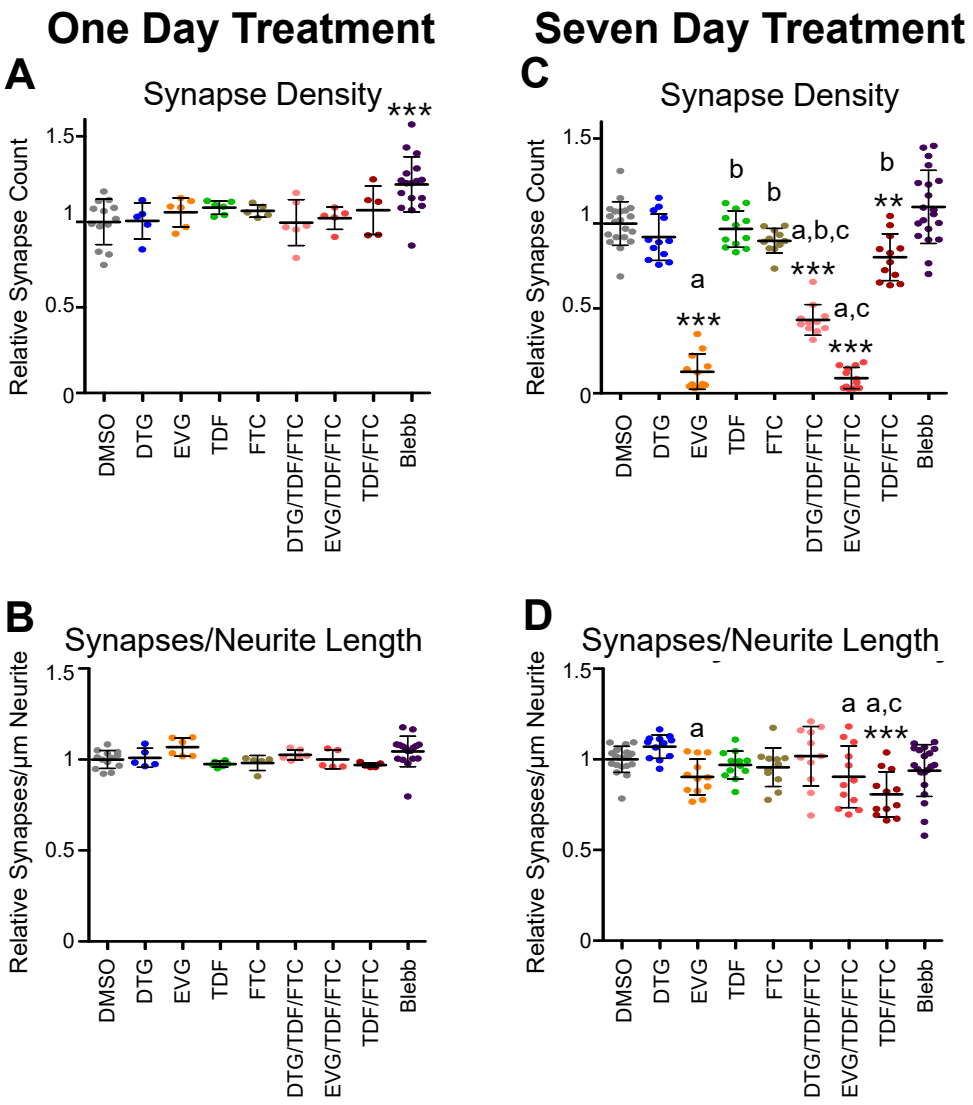

bioRxiv preprint doi: https://doi.org/10.1101/2020.09.05.284422; this version posted January 11, 2021. The copyright holder for this preprint (which was not certified by peer review) is the author/funder, who has granted bioRxiv a license to display the preprint in perpetuity. It is made available under aCC-BY-NC-ND 4.0 International license.

Figure 5

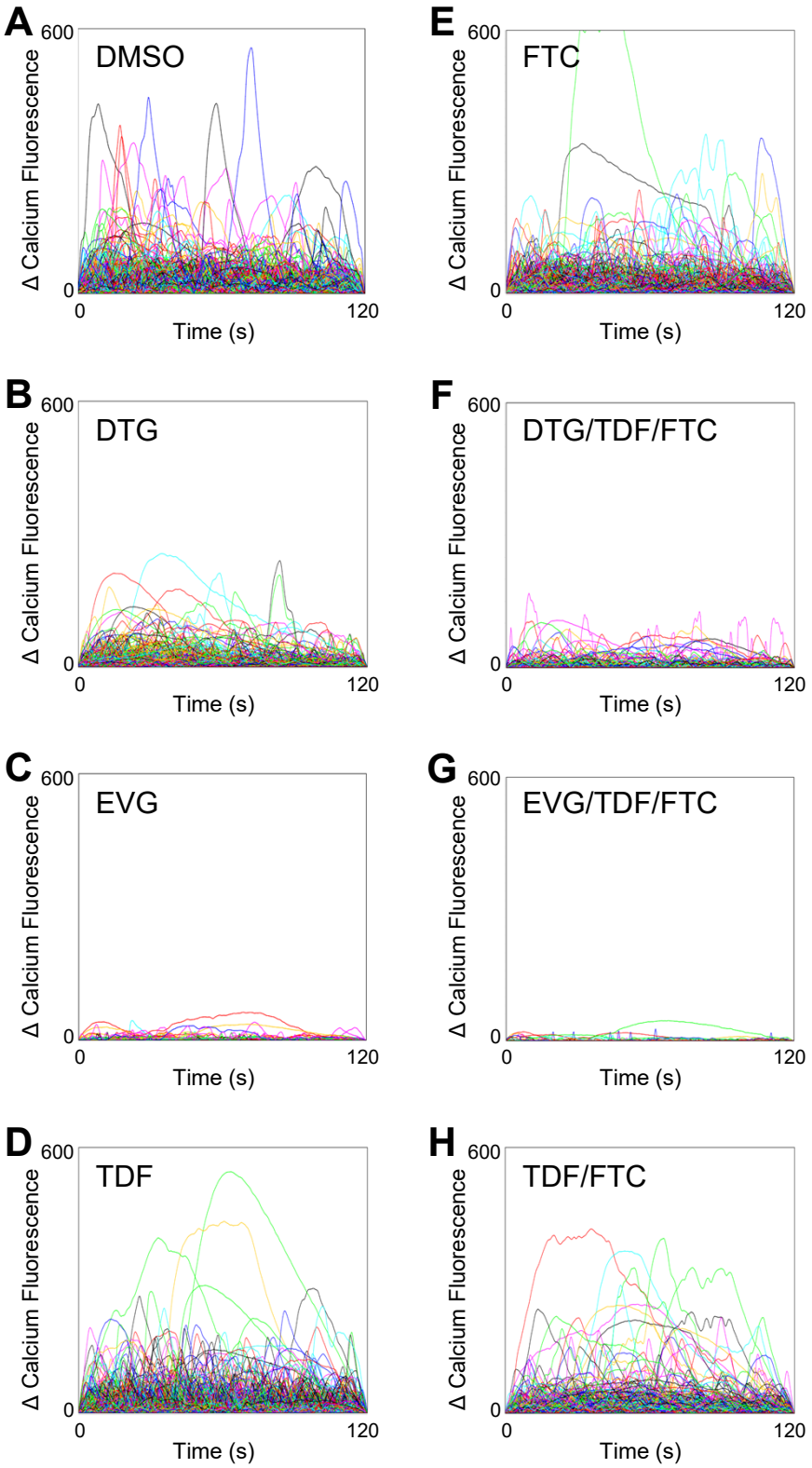

bioRxiv preprint doi: https://doi.org/10.1101/2020.09.05.284422; this version posted January 11, 2021. The copyright holder for this preprint (which was not certified by peer review) is the author/funder, who has granted bioRxiv a license to display the preprint in perpetuity. It is made available under aCC-BY-NC-ND 4.0 International license.

Figure 6

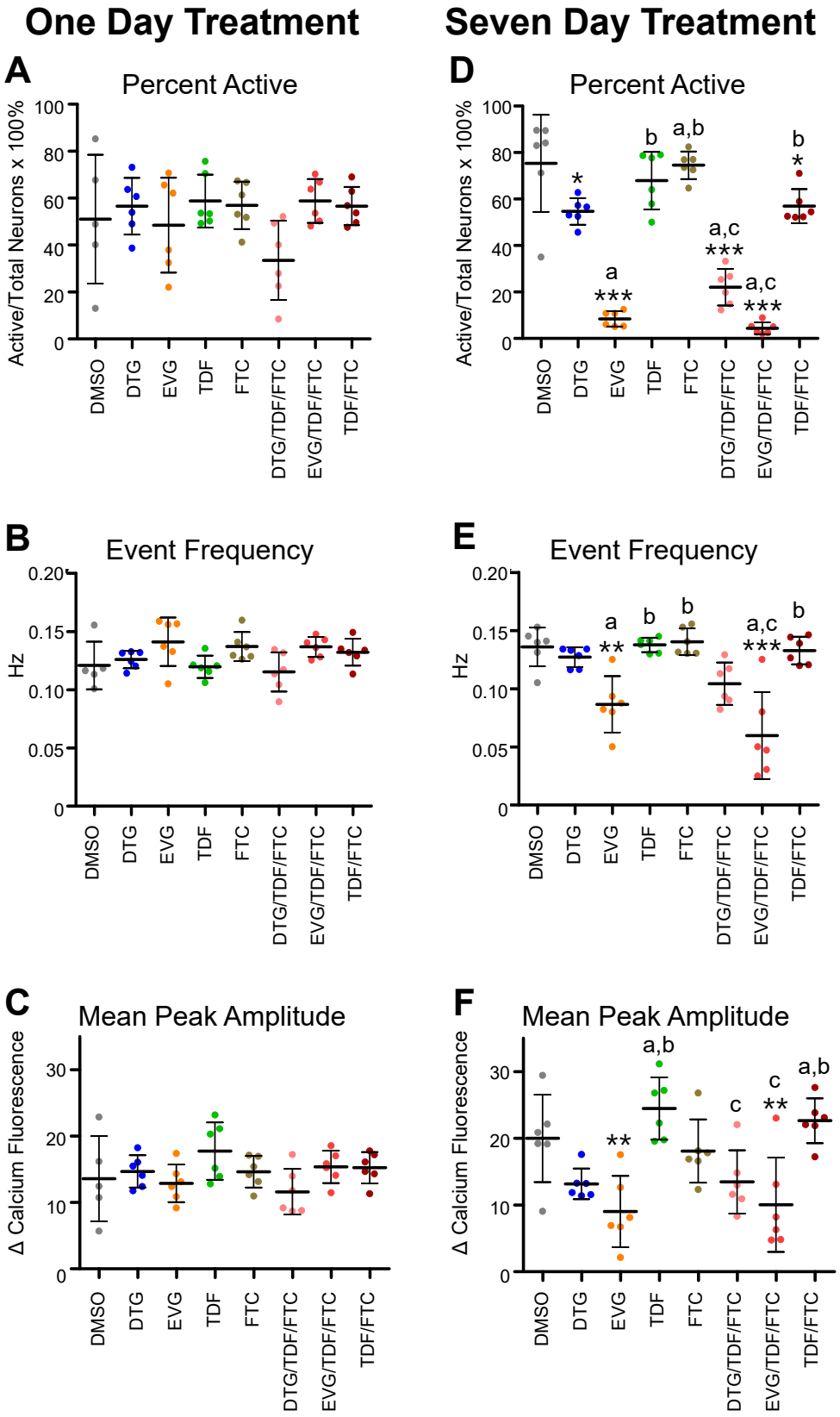

bioRxiv preprint doi: https://doi.org/10.1101/2020.09.05.284422; this version posted January 11, 2021. The copyright holder for this preprint (which was not certified by peer review) is the author/funder, who has granted bioRxiv a license to display the preprint in perpetuity. It is made available under aCC-BY-NC-ND 4.0 International license.

Figure 7

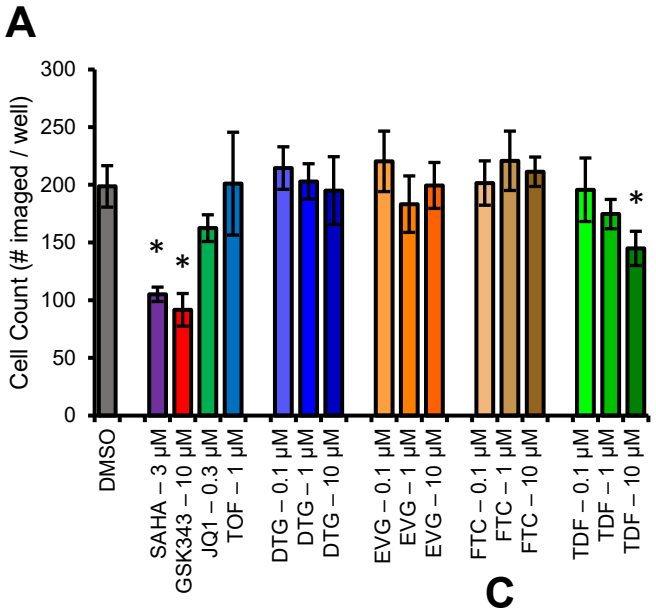

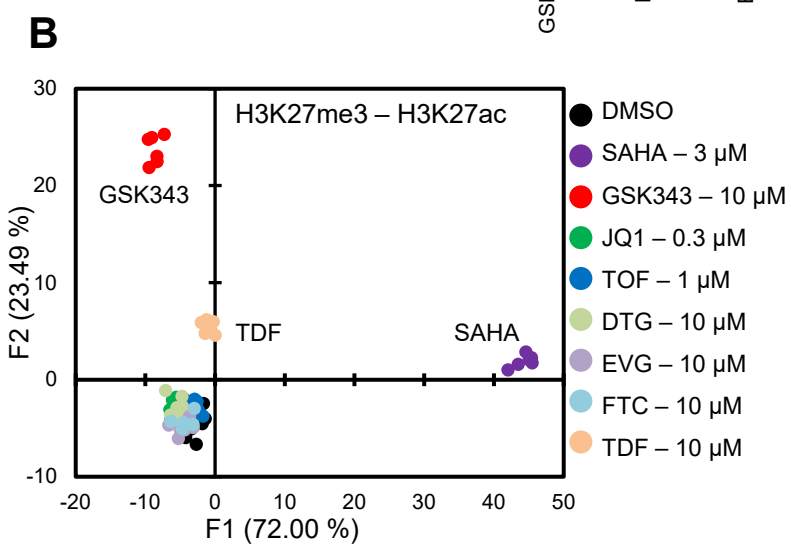

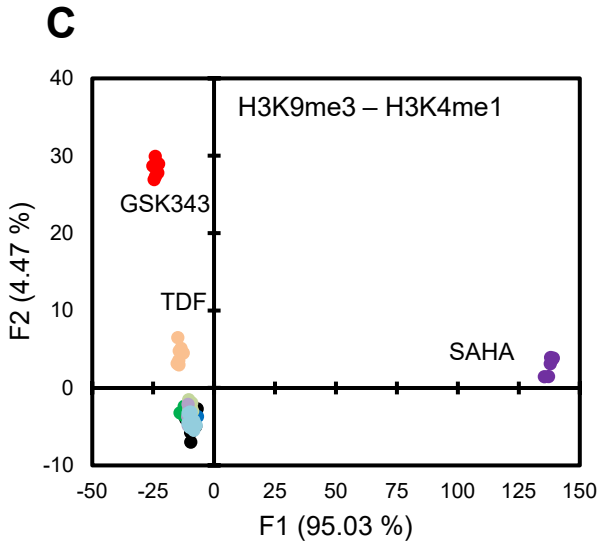

D

	DMSO	GSK343 - 10uM	SAHA - 3uM	JQ1 - 0.3uM	TOF - 1uM	DTG - 10uM	EVG - 10uM	FTC - 10uM	TDF - 10uM
DMSO	33.3	0.0	0.0	0.0	16.7	16.7	16.7	16.7	0.0
GSK343 - 10uM	0.0	100.0	0.0	0.0	0.0	0.0	0.0	0.0	0.0
SAHA - 3uM	0.0	0.0	100.0	0.0	0.0	0.0	0.0	0.0	0.0
JQ1 - 0.3uM	0.0	0.0	0.0	33.3	0.0	0.0	33.3	33.3	0.0
TOF - 1uM	33.3	0.0	0.0	0.0	0.0	0.0	0.0	66.7	0.0
DTG - 10uM	66.7	0.0	0.0	0.0	0.0	0.0	0.0	33.3	0.0
EVG - 10uM	33.3	0.0	0.0	33.3	0.0	33.3	0.0	0.0	0.0
FTC - 10uM	33.3	0.0	0.0	0.0	0.0	33.3	0.0	33.3	0.0
TDF - 10uM	0.0	0.0	0.0	0.0	0.0	0.0	0.0	0.0	100.0

E

	DMSO	GSK343 - 10uM	SAHA - 3uM	JQ1 - 0.3uM	TOF - 1uM	DTG - 10uM	EVG - 10uM	FTC - 10uM	TDF - 10uM
DMSO	83.3	0.0	0.0	0.0	0.0	16.7	0.0	0.0	0.0
GSK343 - 10uM	0.0	100.0	0.0	0.0	0.0	0.0	0.0	0.0	0.0
SAHA - 3uM	0.0	0.0	100.0	0.0	0.0	0.0	0.0	0.0	0.0
JQ1 - 0.3uM	33.3	0.0	0.0	33.3	33.3	0.0	0.0	0.0	0.0
TOF - 1uM	0.0	0.0	0.0	0.0	0.0	33.3	33.3	33.3	0.0
DTG - 10uM	25.0	0.0	0.0	0.0	0.0	25.0	25.0	25.0	0.0
EVG - 10uM	50.0	0.0	0.0	0.0	0.0	0.0	50.0	0.0	0.0
FTC - 10uM	0.0	0.0	0.0	0.0	0.0	25.0	50.0	25.0	0.0
TDF - 10uM	0.0	0.0	0.0	0.0	0.0	0.0	0.0	0.0	100.0

bioRxiv preprint doi: https://doi.org/10.1101/2020.09.05.284422; this version posted January 11, 2021. The copyright holder for this preprint (which was not certified by peer review) is the author/funder, who has granted bioRxiv a license to display the preprint in perpetuity. It is made available under aCC-BY-NC-ND 4.0 International license.

Figure 8

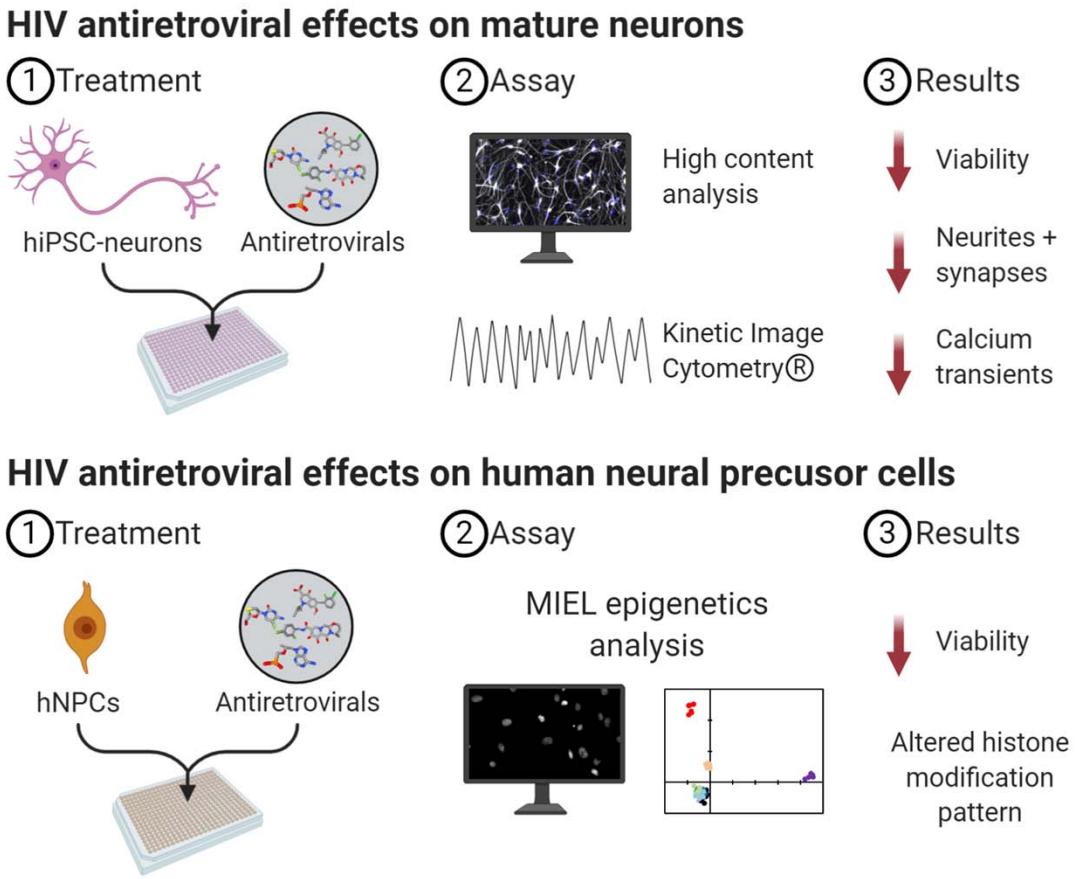

bioRxiv preprint doi: https://doi.org/10.1101/2020.09.05.284422; this version posted January 11, 2021. The copyright holder for this preprint (which was not certified by peer review) is the author/funder, who has granted bioRxiv a license to display the preprint in perpetuity. It is made available under aCC-BY-NC-ND 4.0 International license.

Table S1

Neuronal Viability

One Day Treatment

Tukey's Multiple Comparison Test	Mean Difference	Significance
DMSO vs DTG	-0.002360	ns
DMSO vs EVG	0.02578	ns
DMSO vs TDF	0.002801	ns
DMSO vs FTC	-0.06047	ns
DMSO vs DTG TDF FTC	0.1080	ns
DMSO vs EVG TDF FTC	0.01235	ns
DMSO vs TDF FTC	0.03525	ns
DMSO vs Blebb	-0.02633	ns
DTG vs EVG	0.02814	ns
DTG vs TDF	0.005161	ns
DTG vs FTC	-0.05811	ns
DTG vs DTG TDF FTC	0.1104	ns
DTG vs EVG TDF FTC	0.01471	ns
DTG vs TDF FTC	0.03761	ns
DTG vs Blebb	-0.02397	ns
EVG vs TDF	-0.02298	ns
EVG vs FTC	-0.08625	ns
EVG vs DTG TDF FTC	0.08225	ns
EVG vs EVG TDF FTC	-0.01343	ns
EVG vs TDF FTC	0.009474	ns
EVG vs Blebb	-0.05211	ns
TDF vs FTC	-0.06328	ns
TDF vs DTG TDF FTC	0.1052	ns
TDF vs EVG TDF FTC	0.009544	ns
TDF vs TDF FTC	0.03245	ns
TDF vs Blebb	-0.02913	ns
FTC vs DTG TDF FTC	0.1685	**
FTC vs EVG TDF FTC	0.07282	ns
FTC vs TDF FTC	0.09573	ns
FTC vs Blebb	0.03414	ns
DTG TDF FTC vs EVG TDF FTC	-0.09568	ns
DTG TDF FTC vs TDF FTC	-0.07277	ns
DTG TDF FTC vs Blebb	-0.1344	**
EVG TDF FTC vs TDF FTC	0.02291	ns
EVG TDF FTC vs Blebb	-0.03868	ns
TDF FTC vs Blebb	-0.06158	ns

Seven Day Treatment

Tukey's Multiple Comparison Test	Mean Difference	Significance
DMSO vs DTG	0.1952	***
DMSO vs EVG	0.7947	***
DMSO vs TDF	0.2858	***
DMSO vs FTC	0.009897	ns
DMSO vs DTG TDF FTC	0.6876	***
DMSO vs EVG TDF FTC	0.8388	***
DMSO vs TDF FTC	0.3164	***
DMSO vs Blebb	-0.05650	ns
DTG vs EVG	0.5994	***
DTG vs TDF	0.09056	ns
DTG vs FTC	-0.1853	***
DTG vs DTG TDF FTC	0.4923	***
DTG vs EVG TDF FTC	0.6436	***
DTG vs TDF FTC	0.1212	*
DTG vs Blebb	-0.2517	***
EVG vs TDF	-0.5089	***
EVG vs FTC	-0.7848	***
EVG vs DTG TDF FTC	-0.1071	ns
EVG vs EVG TDF FTC	0.04412	ns
EVG vs TDF FTC	-0.4783	***
EVG vs Blebb	-0.8512	***
TDF vs FTC	-0.2759	***
TDF vs DTG TDF FTC	0.4018	***
TDF vs EVG TDF FTC	0.5530	***
TDF vs TDF FTC	0.03061	ns
TDF vs Blebb	-0.3423	***
FTC vs DTG TDF FTC	0.6777	***
FTC vs EVG TDF FTC	0.8289	***
FTC vs TDF FTC	0.3065	***
FTC vs Blebb	-0.06640	ns
DTG TDF FTC vs EVG TDF FTC	0.1512	***
DTG TDF FTC vs TDF FTC	-0.3712	***
DTG TDF FTC vs Blebb	-0.7441	***
EVG TDF FTC vs TDF FTC	-0.5224	***
EVG TDF FTC vs Blebb	-0.8953	***
TDF FTC vs Blebb	-0.3729	***

bioRxiv preprint doi: https://doi.org/10.1101/2020.09.05.284422; this version posted January 11, 2021. The copyright holder for this preprint (which was not certified by peer review) is the author/funder, who has granted bioRxiv a license to display the preprint in perpetuity. It is made available under aCC-BY-NC-ND 4.0 International license.

Table S2

Total Neurite Length

One Day Treatment

Tukey's Multiple Comparison Test	Mean Difference	Significance
DMSO vs DTG	-0.003525	ns
DMSO vs EVG	0.001910	ns
DMSO vs TDF	-0.1167	ns
DMSO vs FTC	-0.08899	ns
DMSO vs DTG TDF FTC	0.02920	ns
DMSO vs EVG TDF FTC	-0.006731	ns
DMSO vs TDF FTC	-0.09129	ns
DMSO vs Blebb	-0.1680	**
DTG vs EVG	0.005434	ns
DTG vs TDF	-0.1132	ns
DTG vs FTC	-0.08547	ns
DTG vs DTG TDF FTC	0.03272	ns
DTG vs EVG TDF FTC	-0.003206	ns
DTG vs TDF FTC	-0.08777	ns
DTG vs Blebb	-0.1645	ns
EVG vs TDF	-0.1186	ns
EVG vs FTC	-0.09090	ns
EVG vs DTG TDF FTC	0.02729	ns
EVG vs EVG TDF FTC	-0.008641	ns
EVG vs TDF FTC	-0.09320	ns
EVG vs Blebb	-0.1699	*
TDF vs FTC	0.02772	ns
TDF vs DTG TDF FTC	0.1459	ns
TDF vs EVG TDF FTC	0.1100	ns
TDF vs TDF FTC	0.02542	ns
TDF vs Blebb	-0.05132	ns
FTC vs DTG TDF FTC	0.1182	ns
FTC vs EVG TDF FTC	0.08226	ns
FTC vs TDF FTC	-0.002303	ns
FTC vs Blebb	-0.07904	ns
DTG TDF FTC vs EVG TDF FTC	-0.03593	ns
DTG TDF FTC vs TDF FTC	-0.1205	ns
DTG TDF FTC vs Blebb	-0.1972	**
EVG TDF FTC vs TDF FTC	-0.08456	ns
EVG TDF FTC vs Blebb	-0.1613	ns
TDF FTC vs Blebb	-0.07674	ns

Seven Day Treatment

Tukey's Multiple Comparison Test	Mean Difference	Significance
DMSO vs DTG	0.1369	ns
DMSO vs EVG	0.8657	***
DMSO vs TDF	-0.006719	ns
DMSO vs FTC	0.06042	ns
DMSO vs DTG TDF FTC	0.5543	***
DMSO vs EVG TDF FTC	0.9078	***
DMSO vs TDF FTC	0.02082	ns
DMSO vs Blebb	-0.1483	*
DTG vs EVG	0.7288	***
DTG vs TDF	-0.1436	ns
DTG vs FTC	-0.07650	ns
DTG vs DTG TDF FTC	0.4174	***
DTG vs EVG TDF FTC	0.7708	***
DTG vs TDF FTC	-0.1161	ns
DTG vs Blebb	-0.2853	***
EVG vs TDF	-0.8724	***
EVG vs FTC	-0.8053	***
EVG vs DTG TDF FTC	-0.3114	***
EVG vs EVG TDF FTC	0.04204	ns
EVG vs TDF FTC	-0.8449	***
EVG vs Blebb	-1.014	***
TDF vs FTC	0.06714	ns
TDF vs DTG TDF FTC	0.5610	***
TDF vs EVG TDF FTC	0.9145	***
TDF vs TDF FTC	0.02753	ns
TDF vs Blebb	-0.1416	ns
FTC vs DTG TDF FTC	0.4939	***
FTC vs EVG TDF FTC	0.8473	***
FTC vs TDF FTC	-0.03961	ns
FTC vs Blebb	-0.2088	**
DTG TDF FTC vs EVG TDF FTC	0.3535	***
DTG TDF FTC vs TDF FTC	-0.5335	***
DTG TDF FTC vs Blebb	-0.7026	***
EVG TDF FTC vs TDF FTC	-0.8870	***
EVG TDF FTC vs Blebb	-1.056	***
TDF FTC vs Blebb	-0.1691	*

bioRxiv preprint doi: https://doi.org/10.1101/2020.09.05.284422; this version posted January 11, 2021. The copyright holder for this preprint (which was not certified by peer review) is the author/funder, who has granted bioRxiv a license to display the preprint in perpetuity. It is made available under aCC-BY-NC-ND 4.0 International license.

Table S3

Neurite Length Per Neuron

One Day Treatment

Tukey's Multiple Comparison Test	Mean Difference	Significance
DMSO vs DTG	-0.09484	ns
DMSO vs EVG	-0.02655	ns
DMSO vs TDF	-0.1107	ns
DMSO vs FTC	-0.01540	ns
DMSO vs DTG TDF FTC	-0.1021	ns
DMSO vs EVG TDF FTC	-0.02473	ns
DMSO vs TDF FTC	-0.1341	ns
DMSO vs Blebb	-0.1484	ns
DTG vs EVG	0.06828	ns
DTG vs TDF	-0.01582	ns
DTG vs FTC	0.07943	ns
DTG vs DTG TDF FTC	-0.007285	ns
DTG vs EVG TDF FTC	0.07010	ns
DTG vs TDF FTC	-0.03929	ns
DTG vs Blebb	-0.05354	ns
EVG vs TDF	-0.08410	ns
EVG vs FTC	0.01115	ns
EVG vs DTG TDF FTC	-0.07557	ns
EVG vs EVG TDF FTC	0.001821	ns
EVG vs TDF FTC	-0.1076	ns
EVG vs Blebb	-0.1218	ns
TDF vs FTC	0.09526	ns
TDF vs DTG TDF FTC	0.008536	ns
TDF vs EVG TDF FTC	0.08592	ns
TDF vs TDF FTC	-0.02347	ns
TDF vs Blebb	-0.03772	ns
FTC vs DTG TDF FTC	-0.08672	ns
FTC vs EVG TDF FTC	-0.009331	ns
FTC vs TDF FTC	-0.1187	ns
FTC vs Blebb	-0.1330	ns
DTG TDF FTC vs EVG TDF FTC	0.07739	ns
DTG TDF FTC vs TDF FTC	-0.03200	ns
DTG TDF FTC vs Blebb	-0.04625	ns
EVG TDF FTC vs TDF FTC	-0.1094	ns
EVG TDF FTC vs Blebb	-0.1236	ns
TDF FTC vs Blebb	-0.01425	ns

Seven Day Treatment

Tukey's Multiple Comparison Test	Mean Difference	Significance
DMSO vs DTG	-0.02907	ns
DMSO vs EVG	0.2885	ns
DMSO vs TDF	-0.3622	ns
DMSO vs FTC	0.1027	ns
DMSO vs DTG TDF FTC	-0.5172	*
DMSO vs EVG TDF FTC	0.2840	ns
DMSO vs TDF FTC	-0.3790	ns
DMSO vs Blebb	-0.08370	ns
DTG vs EVG	0.3175	ns
DTG vs TDF	-0.3331	ns
DTG vs FTC	0.1317	ns
DTG vs DTG TDF FTC	-0.4881	ns
DTG vs EVG TDF FTC	0.3131	ns
DTG vs TDF FTC	-0.3499	ns
DTG vs Blebb	-0.05463	ns
EVG vs TDF	-0.6507	**
EVG vs FTC	-0.1858	ns
EVG vs DTG TDF FTC	-0.8056	***
EVG vs EVG TDF FTC	-0.004459	ns
EVG vs TDF FTC	-0.6675	**
EVG vs Blebb	-0.3722	ns
TDF vs FTC	0.4649	ns
TDF vs DTG TDF FTC	-0.1550	ns
TDF vs EVG TDF FTC	0.6462	**
TDF vs TDF FTC	-0.01681	ns
TDF vs Blebb	0.2785	ns
FTC vs DTG TDF FTC	-0.6198	*
FTC vs EVG TDF FTC	0.1813	ns
FTC vs TDF FTC	-0.4817	ns
FTC vs Blebb	-0.1864	ns
DTG TDF FTC vs EVG TDF FTC	0.8012	***
DTG TDF FTC vs TDF FTC	0.1382	ns
DTG TDF FTC vs Blebb	0.4335	ns
EVG TDF FTC vs TDF FTC	-0.6630	**
EVG TDF FTC vs Blebb	-0.3677	ns
TDF FTC vs Blebb	0.2953	ns

bioRxiv preprint doi: https://doi.org/10.1101/2020.09.05.284422; this version posted January 11, 2021. The copyright holder for this preprint (which was not certified by peer review) is the author/funder, who has granted bioRxiv a license to display the preprint in perpetuity. It is made available under aCC-BY-NC-ND 4.0 International license.

Table S4

Synapse Density

One Day Treatment

Tukey's Multiple Comparison Test	Mean Difference	Significance
DMSO vs DTG	-0.005561	ns
DMSO vs EVG	-0.05608	ns
DMSO vs TDF	-0.08320	ns
DMSO vs FTC	-0.06424	ns
DMSO vs DTG TDF FTC	0.004011	ns
DMSO vs EVG TDF FTC	-0.02199	ns
DMSO vs TDF FTC	-0.06814	ns
DMSO vs Blebb	-0.2197	***
DTG vs EVG	-0.05051	ns
DTG vs TDF	-0.07764	ns
DTG vs FTC	-0.05868	ns
DTG vs DTG TDF FTC	0.009572	ns
DTG vs EVG TDF FTC	-0.01643	ns
DTG vs TDF FTC	-0.06258	ns
DTG vs Blebb	-0.2142	*
EVG vs TDF	-0.02713	ns
EVG vs FTC	-0.008162	ns
EVG vs DTG TDF FTC	0.06009	ns
EVG vs EVG TDF FTC	0.03408	ns
EVG vs TDF FTC	-0.01207	ns
EVG vs Blebb	-0.1636	ns
TDF vs FTC	0.01897	ns
TDF vs DTG TDF FTC	0.08722	ns
TDF vs EVG TDF FTC	0.06121	ns
TDF vs TDF FTC	0.01506	ns
TDF vs Blebb	-0.1365	ns
FTC vs DTG TDF FTC	0.06825	ns
FTC vs EVG TDF FTC	0.04225	ns
FTC vs TDF FTC	-0.003904	ns
FTC vs Blebb	-0.1555	ns
DTG TDF FTC vs EVG TDF FTC	-0.02600	ns
DTG TDF FTC vs TDF FTC	-0.07215	ns
DTG TDF FTC vs Blebb	-0.2237	**
EVG TDF FTC vs TDF FTC	-0.04615	ns
EVG TDF FTC vs Blebb	-0.1977	ns
TDF FTC vs Blebb	-0.1516	ns

Seven Day Treatment

Tukey's Multiple Comparison Test	Mean Difference	Significance
DMSO vs DTG	0.07950	ns
DMSO vs EVG	0.8726	***
DMSO vs TDF	0.03189	ns
DMSO vs FTC	0.1014	ns
DMSO vs DTG TDF FTC	0.5669	***
DMSO vs EVG TDF FTC	0.9095	***
DMSO vs TDF FTC	0.1984	**
DMSO vs Blebb	-0.09814	ns
DTG vs EVG	0.7931	***
DTG vs TDF	-0.04760	ns
DTG vs FTC	0.02194	ns
DTG vs DTG TDF FTC	0.4874	***
DTG vs EVG TDF FTC	0.8300	***
DTG vs TDF FTC	0.1189	ns
DTG vs Blebb	-0.1776	*
EVG vs TDF	-0.8407	***
EVG vs FTC	-0.7711	***
EVG vs DTG TDF FTC	-0.3056	***
EVG vs EVG TDF FTC	0.03694	ns
EVG vs TDF FTC	-0.6742	***
EVG vs Blebb	-0.9707	***
TDF vs FTC	0.06954	ns
TDF vs DTG TDF FTC	0.5350	***
TDF vs EVG TDF FTC	0.8776	***
TDF vs TDF FTC	0.1665	ns
TDF vs Blebb	-0.1300	ns
FTC vs DTG TDF FTC	0.4655	***
FTC vs EVG TDF FTC	0.8081	***
FTC vs TDF FTC	0.09693	ns
FTC vs Blebb	-0.1996	**
DTG TDF FTC vs EVG TDF FTC	0.3426	***
DTG TDF FTC vs TDF FTC	-0.3685	***
DTG TDF FTC vs Blebb	-0.6651	***
EVG TDF FTC vs TDF FTC	-0.7111	***
EVG TDF FTC vs Blebb	-1.008	***
TDF FTC vs Blebb	-0.2965	***

bioRxiv preprint doi: https://doi.org/10.1101/2020.09.05.284422; this version posted January 11, 2021. The copyright holder for this preprint (which was not certified by peer review) is the author/funder, who has granted bioRxiv a license to display the preprint in perpetuity. It is made available under aCC-BY-NC-ND 4.0 International license.

Table S5

Synapses/Neurite Length

One Day Treatment

Tukey's Multiple Comparison Test	Mean Difference	Significance
DMSO vs DTG	-0.009334	ns
DMSO vs EVG	-0.06784	ns
DMSO vs TDF	0.02567	ns
DMSO vs FTC	0.01931	ns
DMSO vs DTG TDF FTC	-0.02523	ns
DMSO vs EVG TDF FTC	-0.0004753	ns
DMSO vs TDF FTC	0.03048	ns
DMSO vs Blebb	-0.04413	ns
DTG vs EVG	-0.05851	ns
DTG vs TDF	0.03500	ns
DTG vs FTC	0.02864	ns
DTG vs DTG TDF FTC	-0.01589	ns
DTG vs EVG TDF FTC	0.008858	ns
DTG vs TDF FTC	0.03981	ns
DTG vs Blebb	-0.03480	ns
EVG vs TDF	0.09351	ns
EVG vs FTC	0.08715	ns
EVG vs DTG TDF FTC	0.04262	ns
EVG vs EVG TDF FTC	0.06737	ns
EVG vs TDF FTC	0.09832	ns
EVG vs Blebb	0.02371	ns
TDF vs FTC	-0.006361	ns
TDF vs DTG TDF FTC	-0.05090	ns
TDF vs EVG TDF FTC	-0.02615	ns
TDF vs TDF FTC	0.004810	ns
TDF vs Blebb	-0.06980	ns
FTC vs DTG TDF FTC	-0.04454	ns
FTC vs EVG TDF FTC	-0.01979	ns
FTC vs TDF FTC	0.01117	ns
FTC vs Blebb	-0.06344	ns
DTG TDF FTC vs EVG TDF FTC	0.02475	ns
DTG TDF FTC vs TDF FTC	0.05571	ns
DTG TDF FTC vs Blebb	-0.01891	ns
EVG TDF FTC vs TDF FTC	0.03096	ns
EVG TDF FTC vs Blebb	-0.04366	ns
TDF FTC vs Blebb	-0.07461	ns

Seven Day Treatment

Tukey's Multiple Comparison Test	Mean Difference	Significance
DMSO vs DTG	-0.07061	ns
DMSO vs EVG	0.09677	ns
DMSO vs TDF	0.03095	ns
DMSO vs FTC	0.04279	ns
DMSO vs DTG TDF FTC	-0.01777	ns
DMSO vs EVG TDF FTC	0.09549	ns
DMSO vs TDF FTC	0.1925	***
DMSO vs Blebb	0.06131	ns
DTG vs EVG	0.1674	*
DTG vs TDF	0.1016	ns
DTG vs FTC	0.1134	ns
DTG vs DTG TDF FTC	0.05284	ns
DTG vs EVG TDF FTC	0.1661	*
DTG vs TDF FTC	0.2632	***
DTG vs Blebb	0.1319	ns
EVG vs TDF	-0.06582	ns
EVG vs FTC	-0.05398	ns
EVG vs DTG TDF FTC	-0.1145	ns
EVG vs EVG TDF FTC	-0.001282	ns
EVG vs TDF FTC	0.09577	ns
EVG vs Blebb	-0.03546	ns
TDF vs FTC	0.01184	ns
TDF vs DTG TDF FTC	-0.04872	ns
TDF vs EVG TDF FTC	0.06454	ns
TDF vs TDF FTC	0.1616	*
TDF vs Blebb	0.03036	ns
FTC vs DTG TDF FTC	-0.06056	ns
FTC vs EVG TDF FTC	0.05270	ns
FTC vs TDF FTC	0.1497	ns
FTC vs Blebb	0.01852	ns
DTG TDF FTC vs EVG TDF FTC	0.1133	ns
DTG TDF FTC vs TDF FTC	0.2103	**
DTG TDF FTC vs Blebb	0.07909	ns
EVG TDF FTC vs TDF FTC	0.09705	ns
EVG TDF FTC vs Blebb	-0.03418	ns
TDF FTC vs Blebb	-0.1312	ns

bioRxiv preprint doi: https://doi.org/10.1101/2020.09.05.284422; this version posted January 11, 2021. The copyright holder for this preprint (which was not certified by peer review) is the author/funder, who has granted bioRxiv a license to display the preprint in perpetuity. It is made available under aCC-BY-NC-ND 4.0 International license.

Table S6

Percent Active

One Day Treatment

Tukey's Multiple Comparison Test	Mean Difference	Significance
DMSO vs DTG	-5.503	ns
DMSO vs EVG	2.569	ns
DMSO vs TDF	-7.743	ns
DMSO vs FTC	-5.904	ns
DMSO vs DTG TDF FTC	17.57	ns
DMSO vs EVG TDF FTC	-7.779	ns
DMSO vs TDF FTC	-5.569	ns
DTG vs EVG	8.073	ns
DTG vs TDF	-2.239	ns
DTG vs FTC	-0.4002	ns
DTG vs DTG TDF FTC	23.07	ns
DTG vs EVG TDF FTC	-2.276	ns
DTG vs TDF FTC	-0.06578	ns
EVG vs TDF	-10.31	ns
EVG vs FTC	-8.473	ns
EVG vs DTG TDF FTC	15.00	ns
EVG vs EVG TDF FTC	-10.35	ns
EVG vs TDF FTC	-8.138	ns
TDF vs FTC	1.839	ns
TDF vs DTG TDF FTC	25.31	ns
TDF vs EVG TDF FTC	-0.03650	ns
TDF vs TDF FTC	2.174	ns
FTC vs DTG TDF FTC	23.47	ns
FTC vs EVG TDF FTC	-1.876	ns
FTC vs TDF FTC	0.3345	ns
DTG TDF FTC vs EVG TDF FTC	-25.35	ns
DTG TDF FTC vs TDF FTC	-23.14	ns
EVG TDF FTC vs TDF FTC	2.210	ns

Seven Day Treatment

Tukey's Multiple Comparison Test	Mean Difference	Significance
DMSO vs DTG	20.72	*
DMSO vs EVG	66.99	***
DMSO vs TDF	7.533	ns
DMSO vs FTC	0.8424	ns
DMSO vs DTG TDF FTC	53.36	***
DMSO vs EVG TDF FTC	71.02	***
DMSO vs TDF FTC	18.47	*
DTG vs EVG	46.27	***
DTG vs TDF	-13.19	ns
DTG vs FTC	-19.88	*
DTG vs DTG TDF FTC	32.64	***
DTG vs EVG TDF FTC	50.30	***
DTG vs TDF FTC	-2.247	ns
EVG vs TDF	-59.46	***
EVG vs FTC	-66.15	***
EVG vs DTG TDF FTC	-13.63	ns
EVG vs EVG TDF FTC	4.024	ns
EVG vs TDF FTC	-48.52	***
TDF vs FTC	-6.690	ns
TDF vs DTG TDF FTC	45.83	***
TDF vs EVG TDF FTC	63.48	***
TDF vs TDF FTC	10.94	ns
FTC vs DTG TDF FTC	52.52	***
FTC vs EVG TDF FTC	70.17	***
FTC vs TDF FTC	17.63	ns
DTG TDF FTC vs EVG TDF FTC	17.66	ns
DTG TDF FTC vs TDF FTC	-34.89	***
EVG TDF FTC vs TDF FTC	-52.55	***

bioRxiv preprint doi: https://doi.org/10.1101/2020.09.05.284422; this version posted January 11, 2021. The copyright holder for this preprint (which was not certified by peer review) is the author/funder, who has granted bioRxiv a license to display the preprint in perpetuity. It is made available under aCC-BY-NC-ND 4.0 International license.

Table S7

Event Frequency

One Day Treatment

Tukey's Multiple Comparison Test	Mean Difference	Significance
DMSO vs DTG	-0.004991	ns
DMSO vs EVG	-0.02025	ns
DMSO vs TDF	0.001156	ns
DMSO vs FTC	-0.01612	ns
DMSO vs DTG TDF FTC	0.005613	ns
DMSO vs EVG TDF FTC	-0.01591	ns
DMSO vs TDF FTC	-0.01128	ns
DTG vs EVG	-0.01526	ns
DTG vs TDF	0.006147	ns
DTG vs FTC	-0.01113	ns
DTG vs DTG TDF FTC	0.01060	ns
DTG vs EVG TDF FTC	-0.01092	ns
DTG vs TDF FTC	-0.006288	ns
EVG vs TDF	0.02141	ns
EVG vs FTC	0.004131	ns
EVG vs DTG TDF FTC	0.02587	ns
EVG vs EVG TDF FTC	0.004345	ns
EVG vs TDF FTC	0.008976	ns
TDF vs FTC	-0.01728	ns
TDF vs DTG TDF FTC	0.004456	ns
TDF vs EVG TDF FTC	-0.01707	ns
TDF vs TDF FTC	-0.01244	ns
FTC vs DTG TDF FTC	0.02174	ns
FTC vs EVG TDF FTC	0.0002133	ns
FTC vs TDF FTC	0.004844	ns
DTG TDF FTC vs EVG TDF FTC	-0.02152	ns
DTG TDF FTC vs TDF FTC	-0.01689	ns
EVG TDF FTC vs TDF FTC	0.004631	ns

Seven Day Treatment

Tukey's Multiple Comparison Test	Mean Difference	Significance
DMSO vs DTG	0.008768	ns
DMSO vs EVG	0.04941	**
DMSO vs TDF	-0.001770	ns
DMSO vs FTC	-0.004350	ns
DMSO vs DTG TDF FTC	0.03159	ns
DMSO vs EVG TDF FTC	0.07615	***
DMSO vs TDF FTC	0.003081	ns
DTG vs EVG	0.04064	*
DTG vs TDF	-0.01054	ns
DTG vs FTC	-0.01312	ns
DTG vs DTG TDF FTC	0.02282	ns
DTG vs EVG TDF FTC	0.06738	***
DTG vs TDF FTC	-0.005688	ns
EVG vs TDF	-0.05118	**
EVG vs FTC	-0.05376	***
EVG vs DTG TDF FTC	-0.01782	ns
EVG vs EVG TDF FTC	0.02674	ns
EVG vs TDF FTC	-0.04633	**
TDF vs FTC	-0.002579	ns
TDF vs DTG TDF FTC	0.03336	ns
TDF vs EVG TDF FTC	0.07792	***
TDF vs TDF FTC	0.004851	ns
FTC vs DTG TDF FTC	0.03594	*
FTC vs EVG TDF FTC	0.08050	***
FTC vs TDF FTC	0.007430	ns
DTG TDF FTC vs EVG TDF FTC	0.04456	**
DTG TDF FTC vs TDF FTC	-0.02851	ns
EVG TDF FTC vs TDF FTC	-0.07307	***

bioRxiv preprint doi: https://doi.org/10.1101/2020.09.05.284422; this version posted January 11, 2021. The copyright holder for this preprint (which was not certified by peer review) is the author/funder, who has granted bioRxiv a license to display the preprint in perpetuity. It is made available under aCC-BY-NC-ND 4.0 International license.

Table S8

Mean Peak Amplitude

One Day Treatment

Tukey's Multiple Comparison Test	Mean Difference	Significance
DMSO vs DTG	-1.099	ns
DMSO vs EVG	0.6888	ns
DMSO vs TDF	-4.173	ns
DMSO vs FTC	-1.063	ns
DMSO vs DTG TDF FTC	1.968	ns
DMSO vs EVG TDF FTC	-1.797	ns
DMSO vs TDF FTC	-1.659	ns
DTG vs EVG	1.787	ns
DTG vs TDF	-3.074	ns
DTG vs FTC	0.03589	ns
DTG vs DTG TDF FTC	3.066	ns
DTG vs EVG TDF FTC	-0.6987	ns
DTG vs TDF FTC	-0.5604	ns
EVG vs TDF	-4.862	ns
EVG vs FTC	-1.752	ns
EVG vs DTG TDF FTC	1.279	ns
EVG vs EVG TDF FTC	-2.486	ns
EVG vs TDF FTC	-2.348	ns
TDF vs FTC	3.110	ns
TDF vs DTG TDF FTC	6.140	ns
TDF vs EVG TDF FTC	2.375	ns
TDF vs TDF FTC	2.514	ns
FTC vs DTG TDF FTC	3.030	ns
FTC vs EVG TDF FTC	-0.7346	ns
FTC vs TDF FTC	-0.5963	ns
DTG TDF FTC vs EVG TDF FTC	-3.765	ns
DTG TDF FTC vs TDF FTC	-3.627	ns
EVG TDF FTC vs TDF FTC	0.1383	ns

Seven Day Treatment

Tukey's Multiple Comparison Test	Mean Difference	Significance
DMSO vs DTG	6.825	ns
DMSO vs EVG	10.96	*
DMSO vs TDF	-4.487	ns
DMSO vs FTC	1.877	ns
DMSO vs DTG TDF FTC	6.521	ns
DMSO vs EVG TDF FTC	9.934	*
DMSO vs TDF FTC	-2.649	ns
DTG vs EVG	4.134	ns
DTG vs TDF	-11.31	**
DTG vs FTC	-4.948	ns
DTG vs DTG TDF FTC	-0.3046	ns
DTG vs EVG TDF FTC	3.109	ns
DTG vs TDF FTC	-9.475	*
EVG vs TDF	-15.45	***
EVG vs FTC	-9.082	ns
EVG vs DTG TDF FTC	-4.439	ns
EVG vs EVG TDF FTC	-1.025	ns
EVG vs TDF FTC	-13.61	***
TDF vs FTC	6.364	ns
TDF vs DTG TDF FTC	11.01	*
TDF vs EVG TDF FTC	14.42	***
TDF vs TDF FTC	1.837	ns
FTC vs DTG TDF FTC	4.643	ns
FTC vs EVG TDF FTC	8.056	ns
FTC vs TDF FTC	-4.527	ns
DTG TDF FTC vs EVG TDF FTC	3.413	ns
DTG TDF FTC vs TDF FTC	-9.170	ns
EVG TDF FTC vs TDF FTC	-12.58	**